Title: Brd4-bound enhancers drive critical sex differences in glioblastoma

Running title: Sex-specific dual roles for Brd4 in glioblastoma

Authors: Kfoury N[1,#], Qi Z[2,4,#], Wilkinson MN[2,4], Broestl L[1], Berrett KC[3], Moudgil A[2,4], Sankararaman S[2,4], Chen X[2, 4], Gertz J[3], Mitra RD[2,4,†,*] and Rubin JB[1,5,†, *]

Affiliations:

[1] Department of Pediatrics, School of Medicine, Washington University in St. Louis.

[2] Department of Genetics, School of Medicine, Washington University in St. Louis.

[3] Department of Oncological Sciences, Huntsman Cancer Institute, University of Utah.

[4] Center for Genome Sciences and Systems Biology, Washington University in St. Louis.

[5] Department of Neuroscience, School of Medicine, Washington University in St. Louis.

*Correspondence to: Joshua B. Rubin (Rubin_J@wustl.edu) or Robi D. Mitra (rmitra@wustl.edu)

First co-authors

† Last co-authors

Competing interests: The authors have declared that no conflict of interest exists.

Abstract:

Sex can be an important determinant of cancer phenotype and exploring sex-specific tumor biology holds promise for identifying novel therapeutic targets and new approaches to cancer treatment. In an established model of glioblastoma, we discovered transcriptome-wide sexual dimorphism in gene-expression that was concordant with sex differences in H3K27ac marks, large Brd4-bound enhancer usage, and Brd4 localization to Myc and p53 genomic binding sites. The sex-specific enhancer usage drove sex differences in stem cell function and tumorigenicity. Moreover, male and female GBM cells exhibited opposing responses to pharmacological or genetic inhibition of Brd4. Brd4 knockdown or inhibition decreased male GBM cell clonogenicity and *in vivo* tumorigenesis, while increasing both in female GBM cells. These results were validated in male and female patient-derived GBM cell lines. Thus, for the first time, Brd4 activity is revealed to drive a sexually dimorphic stem cell and tumorigenic phenotype, resulting in diametrically opposite responses to BET inhibition in male and female glioblastoma cells. This has critical implications for the clinical evaluation and use of BET inhibitors.

Statement of significance: Sex-specific Brd4 activity is demonstrated to drive sex differences in GBM and render male and female tumor cells differentially sensitive to BET inhibitors. This has critical implications for clinical use of this class of drugs.

Introduction

Until recently, most basic and clinical research has focused on investigating the factors that influence disease susceptibility and progression without regard to sex. However, a mounting body of evidence has revealed significant sex differences in the incidence, age of onset, and outcome of numerous human diseases. These include cardiovascular diseases, metabolic diseases, asthma, autoimmune diseases, birth defects, neurological diseases, psychiatric disorders, and cancers (1). This preponderance of sex differences in disease incidence and outcome led to the implementation of new guidelines by the NIH regarding inclusion of sex as a biological variable in all research.

Glioblastoma (GBM), the most common, aggressive, and incurable form of brain cancer (2, 3), is more common in males regardless of race or region of the world (male to female incidence of 1.6:1) (4-7). This sex difference extends across species; a male prevalence also occurs in spontaneous GBM in large dogs suggesting a fundamental effect of sex on GBM risk (8). In addition to the sex difference in GBM incidence, a recent study by Ostrom et al. also documented a significant survival advantage for female GBM patients (9). The reasons for sex differences in GBM incidence and outcome are largely unknown. Our work has primarily focused on studying these sex differences in GBM phenotype as a tool to better understand cancer risk and progression and ultimately develop sex-specific therapies to improve patient survival. While sex differences in disease are often mediated through acute sex hormone actions, sex differences in the rates of multiple kinds of brain tumors are evident at all ages, suggesting that factors other than circulating sex hormones must frequently underlie this discrepancy (10). Such factors may include the organizational or epigenetic effects of transient *in utero* sex hormones or the extra-gonadal effects of sex chromosome encoded genes. We discovered that an established model of GBM involving combined loss of neurofibromin (NF1) and p53 function in murine neocortical astrocytes exhibits

sex differences in *in vivo* tumorigenicity (11, 12) , cell cycle regulation (11, 12), gene expression (11), and chemotherapy response (11) that mimic those observed in GBM patients (11, 12). Together, the human and mouse data suggest that male and female GBM cells may be differentially vulnerable to oncogenic events and to the cytotoxic effects of chemotherapy.

Importantly, in a recent multi-institutional study, we showed that survival for male and female GBM patients after standard surgery, radiation and chemotherapy is dependent upon different transcriptional programs (13). Moreover, we were able to discern multiple sex-specific transcriptional subtypes of GBM that correlated with survival in a sex-specific manner. We hypothesized that these sex-specific transcriptional states would arise through sex-specific epigenetics analogous to mechanisms that drive normal sexual differentiation (14, 15).

Bromodomain and extra-terminal (BET) family proteins are epigenetic readers of histone lysine acetylation and function as co-activators or co-repressors of gene expression by recruiting specific transcriptional complexes to target genes (16). The BET family member Brd4 is essential for regulating transcriptome-wide gene expression and specifying cell identity, including that of GBM. Additionally, Brd4 is an emerging drug target for epigenetic interventions (16-27). Here, we show that sex differences in tumor phenotype arise through differential Brd4-bound enhancer usage in male and female GBM cells. Phenotypic differences between male and female GBM cells are abolished by targeting the BET family proteins either through shRNA knockdown or using a panel of BET inhibitors currently in clinical trials (28, 29). Genetic depletion of individual BET family members indicated that these effects are indeed primarily mediated by the epigenetic reader Brd4. Furthermore, we identify a number of enriched transcription factors at sex-specific Brd4-bound enhancers that could be responsible for mediating these sex differences in the tumorigenic phenotype. Critically important, we demonstrate that treatment with BET inhibitors decreases

clonogenicity and tumorigenicity in male GBM cells while increasing them in female GBM cells. This effect is likely a consequence of sex-specific localization of Brd4 to regulators of stem cell function. Understanding the extent to which sex differences in GBM are mediated by epigenetic mechanisms will be imperative to understanding the biology of sex differences in GBM, stratifying patients for treatment with epigenetic agents, and anticipating potential sex-specific toxicities following systemic disruption of epigenetics.

Results

Male and female GBM cells utilize different sets of Brd4-bound enhancers

Previously, we reported correlations between sex differences in tumorigenicity and gene expression in a murine model of GBM (11, 12). Fifty percent of the sex-based differences in gene expression in the mouse model were concordantly expressed in a sex-specific fashion in human GBM patient gene expression data (11). This was a statistically significant degree of concordance. In addition, we found correlations between sex differences in survival and gene expression in patients with GBM (13). We therefore sought to determine whether these distinct GBM transcriptional states were the product of sex-specific epigenetics and enhancer activity. We prioritized Brd4-bound enhancers for analysis as these enhancers have been shown to play key roles in establishing cell identity (22-27) and thus, we hypothesized, might be operative in establishing cell intrinsic sex differences like those we had observed. Brd4 is an epigenetic reader that binds acetylated histones H3 and H4 throughout the entire cell cycle and is known to be deregulated in numerous cancers (30). Brd4 is thought to play a central role in cancer by promoting epithelial-to-mesenchymal transition, stem cell-like conversion, and pluripotency (19, 20, 31), and

the pharmacological inhibition of this protein has shown therapeutic activity in a number of different cancer models (28, 32-35). To evaluate a potential role for Brd4 in mediating sex differences in GBM, we mapped Brd4 genomic localization in male and female GBM astrocytes (highly active Brd4-bound enhancers and typical Brd4-bound enhancers) using transposon Calling Cards (36, 37) to identify enhancers differentially bound by Brd4. To do so, we fused the piggyBac (PB) transposase to the C terminus of the Brd4 protein, endowing it with the ability to direct the insertion of the PB transposon into the genome close to Brd4 binding sites. Five biological replicates were carried out, and the correlation between replicates was $r > 0.9$ for all pairwise comparisons **(Supplementary Figure 1A)**. Using this protocol, we mapped ~70,000 unique insertions directed by the Brd4-PBase fusion for each male and female sample. Since Brd4 is an epigenetic reader of the acetylated K27 residue of histone H3 (H3K27ac), we confirmed that these newly identified Brd4-bound enhancers were also enriched for H3K27ac. We performed H3K27ac Chromatin Immunoprecipitation Sequencing (ChIP-seq) in male and female GBM cells to identify the genomic regions enriched for this well-known marker of active enhancers (38). Three biological replicates were carried out and the correlation between replicates was $r > 0.9$ for all pairwise comparisons **(Supplementary Figure 1B)**. As expected, data collected from calling cards and H3K27ac ChIP-seq revealed a high concordance between Brd4-bound enhancers and H3K27ac enrichment. A representative example of concordant Brd4 binding and H3K27ac in male and female GBM astrocytes at high and low-enriched regions is depicted in **Figure 1A**. We next analyzed the distances from Brd4 binding sites to the nearest H3K27ac-enriched regions. As shown in **Figure 1B and C**, Brd4 binding sites are significantly enriched at H3K27ac candidate enhancer regions and display concordant gene expression levels indicative of active Brd4-bound

enhancers ($p < 0.01$). More specifically, 82% and 81% of Brd4 bound enhancers were localized within 200bp of H3K27ac peaks in male and female GBM cells, respectively.

Having established that our genomic data is reproducible and that Brd4 binding sites occur at genomic regions enriched for H3K27ac, we next sought to identify the genomic loci that are differentially bound by Brd4 in male and female cells. We identified 3014 enhancers (13% of all Brd4-bound enhancers in male GBM cells) that bound significantly more Brd4 protein in males and 3122 enhancers (13.5% of all Brd4-bound enhancers in female GBM cells) that bound significantly more Brd4 protein in females **(Figure 2A)**. The Brd4 signal intensity for these enhancers in male and female GBM astrocytes is depicted in **Figure 2B**. Genomic loci that bound Brd4 in a sex-specific manner also displayed sex specific enrichment of H3K27ac (**Figure 2C**). Chromosome location analysis for these sex-specific Brd4-bound enhancers revealed that only 0.13% and 3.11% of male-specific Brd4-bound enhancers are located on the Y and X chromosomes, respectively; whereas 4.29% of female-specific Brd4-bound enhancers are located on the X chromosome, indicating that the observed differences in Brd4-bound enhancers are not simply due to differential Brd4 enhancer enrichment on sex chromosomes. Representative examples of two biologically relevant loci, Nkx2.1 and Zic1/4, which correspond to male-specific and female-specific Brd4-bound enhancer regions respectively, are depicted in **Figure 2D and 2E**. Interestingly, Nkx2.1 has been shown to function both as a "lineage survival" oncogene and tumor suppressor in lung adenocarcinomas, (39, 40) whereas Zic1 is shown to act as a tumor suppressor in breast and thyroid cancers (41, 42), further affirming the potential context-dependent dual role of Brd4 in oncogenesis. This is the first demonstration of differential Brd4-bound enhancer usage by male and female cells of any kind, and suggests that these enhancers may function in sexual

differentiation in a manner similar to their role in determining cell identity and fate (22-24, 27, 43).

We next sought to identify the genes regulated by these sex-specific Brd4-bound enhancers. It is often challenging to reliably link enhancers to the genes they regulate (44), so we used conservative criteria: we linked enhancers to the nearest gene within a 5kb genomic distance. This analysis revealed 1740 male-specific genes and 1604 female-specific genes. Pathway enrichment analysis using Genomatix Pathway System (GePS) on male-specific genes regulated by these sex-specific Brd4-bound enhancers revealed functional enrichment for glioblastoma, cell proliferation, cell cycle, tumor angiogenesis and cancer stem cells. Similar analysis on female-specific genes showed an enrichment in pathways involved in cell differentiation, glioblastoma, regulation of transcription, cell migration and neural stem cells **(Supplementary Table 1)**.

Based on our observation of sex-specific Brd4-bound enhancer usage between male and female GBM cells, we sought to characterize the male and female transcriptomes. We profiled male and female GBM cells with RNA sequencing (RNA-seq). For each condition, three biological replicates were performed; the data were highly reproducible (Pearson $r \geq 0.96$ for all pairwise comparisons) (**Supplementary Figure 1C and D**) and indicated differential expression of 3846 transcripts (FDR < 0.05). We next integrated the male and female-specific Brd4 regulated genes with the differentially expressed genes between male and female GBM astrocytes and narrowed the list of differentially regulated sex-specific Brd4-bound genes to 1118, of which 49.2% are male-specific and 50.8% are female-specific Brd4-regulated genes. A heatmap depiction of the top 400 differentially regulated sex-specific Brd4-bound genes is presented in **Figure 2F**. Pathway enrichment analysis for the 1118 differentially regulated sex-specific Brd4-bound genes was performed using a combination of KEGG pathway and Genomatix Pathway System (GePS).

Classification of these genes according to function revealed a significant number of relevant and important pathways including cell differentiation, glioblastoma, cell proliferation, cell migration and invasion, tumor angiogenesis, stem cell functions and DNA binding-transcription factors **(Figure 2G)**. Thus, global differences in male and female GBM cell transcriptomes in cancer relevant pathways are likely to arise from sex-specific Brd4-bound enhancer activity.

BET family protein (Brd4) depletion/inhibition has opposing effects on clonogenicity in male and female GBM astrocytes

To further validate the transcriptional activation of sex-specific regulatory genes and networks by Brd4-bound enhancers, we performed genetic depletion of the individual BET family members. We used shRNAs specific to either Brd2, Brd3 or Brd4 and then evaluated the effect on the tumorigenic phenotype of male and female GBM cells. 5 different shRNAs specific to each of the Brd family members were evaluated. The shRNAs with the most robust knockdown of each transcript were used for the downstream functional experiments. Brd2, 3 and 4 mRNA levels were partially depleted in male and female GBM cells after infection with the corresponding lentiviral shRNAs (**Figure 3A**). Knockdown of Brd2 did not affect clonogenic frequency in either male or female cells as measured by the extreme limiting dilution assay (ELDA) (**Figure 3B**). Interestingly, male GBM cells with knockdown of Brd4 exhibited a decrease in clonogenic frequency whereas female cells displayed an increase in clonogenic frequency. A similar effect on clonogenic frequency was observed following knockdown of Brd3 in male cells, although it was not as robust as the effect of Brd4 knockdown. Importantly, these strong Brd4 effects were observed despite the more modest knockdown of Brd4 compared to Brd3. Under basal conditions,

male and female GBM cells expressed Brd3 and Brd4 mRNA at similar levels, whereas Brd2 was expressed at higher levels in female cells (*p= 0.02) **(Figure 3C)**.

Based on our observations of sex-specific differences in Brd4 genomic localization and response to Brd4 knockdown between male and female GBM cells, we next sought to investigate whether these GBM astrocytes also exhibit sex-specific treatment response to the Brd4 antagonist JQ1. JQ1 is a thieno-triazolo-1,4-diazepine that displaces Brd4 from chromatin by competitively binding to the acetyl-lysine recognition pocket (28, 32). Treatment of acute myeloid leukemia cells with JQ1 caused a rapid release of Mediator 1 (Med1) from a subset of enhancer regions that were co-occupied by Brd4, leading to a decrease in the expression of neighboring genes (45). We treated male and female GBM cells with either 0.05% DMSO or 500nM JQ1 and then performed extreme limiting dilution assays to measure clonogenic cell frequency. Male cells exhibited greater clonogenic cell activity than female cells under control conditions. Treatment with JQ1 reproducibly abrogated the basal differences in clonogenic frequency between male and female GBM cells by decreasing the clonogenic cell fraction in male cells and increasing the clonogenic cell fraction in female cells **(Figure 3D)**. Taken together, these results demonstrate for the first time that the sex differences in the tumorigenic phenotype we observe in GBM cells are mediated by differential Brd4-bound enhancers, and that the response to JQ1 is sex-dependent.

Given this striking result in the reduction of sex differences in the tumorigenic phenotype with sex-dependent opposing response to Brd4 inhibition with JQ1, we next evaluated all of the BET inhibitors currently in clinical trials for cancer. BET inhibitors are a novel class of epigenetic compounds that selectively target BET proteins and have been shown to have great promise as cancer therapeutics by decreasing cell proliferation and invasion in many cancer types, including GBM (17, 18, 21). However, almost all of the American Type Culture Collection (ATCC) human

cell lines used in the preclinical studies are of male origin and thus, potentially uninformative with regard to sex differences in drug effects. Therefore, we treated male and female GBM astrocytes with a panel of BET inhibitors **(Figure 3E)** that are presently being tested in clinical trials and then performed extreme limiting dilution assays (ELDAs) to measure clonogenic cell frequency. Treatment with BET inhibitors reproducibly decreased clonogenic frequency in male GBM cells while increasing clonogenic frequency in female cells **(Figure 3F)**. Consistent with the Brd2 and Brd3 knockdown results, RVX-208, a BD2 inhibitor with high selectivity to Brd2/3, did not have an effect on clonogenic frequency in male or female GBM cells.

Altogether, these data suggest that Brd4 mediates sex differences in important cancer phenotypes. This has critical implications for targeting Brd4 clinically.

Brd4-bound enhancers regulate sex differences in GBM

To investigate the correlation between sex-specific Brd4-bound enhancers, H3K27ac enrichment and associated gene expression, we compared Brd4 insertions, H3K27ac intensity and the gene expression values in male and female GBM astrocytes for male-specific **(Figure 4A)**, female-specific **(Figure 4B)** and shared **(Figure 4C)** genes. We found that male and female GBM cells have sexually dimorphic Brd4-bound enhancers with concordant H3K27ac intensity and gene expression.

Next, to examine the transcriptional consequences of BET inhibition, we performed RNA-seq on male and female GBM cells treated with JQ1, one of the BET inhibitors that had a strong sex-specific effect on clonogenicity. Briefly, cells were treated with either vehicle (0.05% DMSO) or 500 nM JQ1 for 24 hours, prior to RNA isolation. Gene expression analysis on JQ1 and DMSO treated cells revealed that JQ1 treatment predominantly downregulated gene expression **(Figure 4**

& Supplementary 2A). In addition, genes proximal to Brd4 binding sites were significantly downregulated compared to genes that were distal to Brd4 binding sites (p <0.01), indicating that JQ1 has a specific and directed effect on genes whose expression is driven by Brd4-bound enhancers **(Supplementary Figure 2B).** Pathway analysis for sex-specific Brd4-bound enhancer-associated genes downregulated following JQ1 treatment in male and female GBM cells revealed functionally important pathways such as chromosome aberrations, integrin signaling, and stem cell proliferation, regulated by sex-specific Brd4-bound enhancers in males, and immune system process, cell cycle, and TGF beta signaling, regulated by sex-specific Brd4-bound enhancers in females **(Supplementary Table 2)**.

To begin to understand the mechanism behind the sex-specific stem cell response to BET inhibition, we performed pathway analysis on sex-specific Brd4-bound enhancer genes in male and female GBM astrocytes. Interestingly, male GBM cells were highly enriched for cancer, neoplastic, and pluripotent stem cell pathways, while female GBM cells were mainly enriched for neural stem cell pathways **(Figure 5A)**. Representative examples of these pathways are depicted in **Figure 5B and 5C**. Notably, male-specific genes in stem cell pathways included well-known oncogenes such as Myc, Tet1, and Lif while female-specific genes included tumor suppressors such as Six2 and Six3. Based on these results, we examined the effect JQ1 treatment on the expression of stem cell pathway genes. Because BET inhibition reduced the sex differences in clonogenicity in male and female GBM astrocytes, we hypothesized that baseline gene expression differences in stem cell-related genes would be eliminated by JQ1 treatment. We identified genes with sex differences in expression at baseline that became equivalent following JQ1 treatment and performed pathway analysis. As anticipated, the cancer stem cell pathway was significantly affected by JQ1 treatment. Remarkably, involved male genes were downregulated by JQ1 while

involved female genes were upregulated by JQ1. Overall, there was concordance with the direction of change in gene expression and the decrease and increase in stem cell function in male and female ELDA assays respectively **(Figure 5D)**. These results are indicative of sex-specific transcriptional programs regulated by Brd4-bound enhancers. Identifying which specific pathways are critical to sex differences in GBM will require further functional studies.

BET inhibitors have opposing effects on *in vivo* tumorigenicity in male and female mouse GBM astrocytes

To address the sex-specific effects of BET inhibitor treatment on *in vivo* tumorigenesis, we performed *in vivo* tumor flank implantation studies in female nude mice. Only female nude mice were used as recipient mice for tumor flank implantation since we have previously shown that the sex of the recipient mouse does not affect the *in vivo* growth of implants in this murine model (12). Based on our *in vitro* ELDA studies, we chose to use JQ1 and CPI0610, the two BET inhibitors with the most dramatic sex-specific effect in male and female GBM astrocytes respectively. Each mouse received DMSO, JQ1 or CPI0610 treated male cells (5000 cells) or female cells (1.5 million cells) injected into the flanks. The sex difference in cell dose served to equilibrate the timeframe for the experiment, as female cells produce tumors that grow at a slower rate than male cells. Tumor growth was monitored blindly for 7-12 weeks with thrice weekly micrometer measurements in 3 dimensions. Flank implantation of JQ1-treated male GBM cells was significantly less likely to result in tumor formation than implantation with control DMSO-treated male cells **(Figure 6A, C)**. In contrast, flank implantation of CPI0610-treated female GBM cells was significantly more likely to result in tumor formation than implantation with control DMSO-treated female cells **(Figure 6B, C)**. These results are consistent with the sex-specific effects of

JQ1 and CPI0610 on clonogenic cell frequency in ELDAs, and support a functional change in stem-cell like function following BET inhibitor treatment. Remarkably, this effect was seen following only one dose of BET inhibitor prior to implantation, suggesting that this robust response is maintained and manifested at the epigenetic level. Of note, and as presented in **Figure 3E**, both JQ1 and CPI0610 display a similar pattern in their selectivity to target the different Brd family members, with the highest selectivity for Brd4. Although both drugs had a similar sex-specific directional effect on clonogenic frequency in male and female cells, the magnitude of their effect differed in both the clonogenic cell frequency and *in vivo* tumorigenic assays. A possible explanation for this discrepancy is that the BETi treatment could be affecting different or multiple Brd family members. To rule out this possibility, and to further validate that the sexually dimorphic response to treatment is indeed driven by Brd4, we treated male and female control and Brd4 knockdown cells with either 0.05% DMSO, 500 nM JQ1 or 1 μM CPI0610 and then performed the extreme limited dilution assay to compare clonogenic cell frequency under all the different conditions. No significant change in the effect on clonogenic cell frequency was observed between control and Brd4 knockdown cells treated with BET inhibitors, indicating that Brd4 is the main Brd family member responsible for this sexually dimorphic response to BETi treatment in male and female GBM cells **(Figure 6D)**. Although it is still unclear why we observe different magnitude effects of these two BET_is, the fact that both drugs show a sex-specific effect is notable and predicted by our earlier observations.

Motif analysis at sex-specific Brd4-bound enhancers identified candidate transcription factor drivers of sex differences in the tumorigenic phenotype

Our results suggest that male and female GBM cells have two distinct epigenomes established by the action of Brd4. Inhibiting Brd4 function abrogated sex differences in transcriptional states and the tumorigenic phenotype. Therefore, we conclude that Brd4 has dual functions in cancer, segregated by sex, wherein it acts as an oncogene in male GBM cells and a tumor suppressor in female GBM cells. It has been shown that Brd4 does not bind DNA directly, but is instead recruited to enhancers by transcription factors, either directly, or indirectly though histone acetylation. To better explore the mechanisms underlying this sexual dimorphism in Brd4 function, we performed a motif-based prediction of transcription factor binding sites enriched at sex-specific Brd4-bound enhancers that might be involved in establishing the recruitment of Brd4 to sex-specific genomic loci. Interestingly, transcription factors enriched at male-specific Brd4-bound enhancers included many oncogenes and stem cell markers such as Myc, Klf5 and Oct4 whereas female-specific Brd4-bound enhancers were co-occupied and enriched with transcription factors with tumor suppressor functions such as p53 and Smad4 **(Table 1)**. These results could explain the observed dual functions of Brd4 as an oncogene in male GBM cells and tumor suppressor in female GBM cells.

Sex-specific response to BET inhibition in GBM patient-derived cell lines

Next, we wanted to investigate whether the sex-specific responses to BET inhibition observed in our murine GBM model are also present in human GBM. To do so, we treated male and female human GBM primary cell lines with 005% DMSO, 500 nM JQ1 or 1 μM CPI0610 and then performed the extreme limiting dilution assays to measure clonogenic cell frequency. Consistent with the murine data, treatment with BET_is decreased clonogenic cell frequency in male patient-derived GBM cells while mostly increasing or having no effect on clonogenic cell

frequency in female patient-derived GBM **(Figure 7)**. These results validate the sex-specific effect of BET inhibitor treatment we have observed in the murine GBM cells.

Consequently, we sought to investigate whether sex-specific Brd4-regulated genes also displayed sex-specific concordant expression patterns in human GBM patients. To accomplish this, we mined the RNA-seq expression data for TCGA GBM samples from the cBioPortal and segregated patients by sex (46). Once we identified the genes with differential expression between male and female GBM patients, we crossed these male and female patient gene lists with our mouse differentially expressed male and female sex-specific Brd4-regulated genes. This analysis revealed a concordance in expression differences in 179 out of 771 genes (23.2 %) and 127 out of 887 (14.3%) in male and female sex-specific Brd4-regulated genes, respectively. To validate whether this level of concordance in gene expression between mouse and human GBM samples is not due to chance, we calculated the *p*-values using the cumulative hypergeometric distribution. We found that on average approximately 20.7% and 11.9% of genes in male and female data sets, respectively, would exhibit concordance by chance and the probability of observing a 23.2% and 14.3% concordance in male and female data sets had a *p*-value of 0.045 and 0.016 in male and female, respectively. Hence, we concluded that the observed sex differences in gene expression and Brd4-bound enhancers in our murine GBM model are also representative of sex differences in gene expression that are present in human GBM.

Taken together, these results demonstrate for the first time that the sex differences in GBM cellular phenotypes are mediated by differential Brd4-bound enhancers, and that reduced Brd4 function, either as a consequence of reduced expression or pharmacological inhibition, results in diametrically opposed sex-dependent effects in both mouse models and human patients.

Discussion

Our study demonstrates for the first time that cell intrinsic sex identity is mediated by sex differences in Brd4-bound enhancer usage. In the model utilized here, the differential usage of Brd4-bound enhancers mediated important sex differences in a GBM tumorigenic phenotype. We discovered transcriptome-wide sexual dimorphism in gene-expression, H3K27ac marks and large Brd4-bound enhancers in male and female GBM cells. Brd4 genetic knockdown or pharmacological inhibition with BET_is decreased clonogenicity and tumorigenicity in male cells while increasing clonogenicity in female cells, thus abrogating the sex differences in phenotype. We propose that this sex-dependent response to Brd4 depletion or BET inhibitor treatment is in fact the result of sex differences in Brd4 localization, and specifically in the Brd4-mediated regulation of the stem cell phenotype.

Sex differences in the incidence and severity of numerous human diseases, including cancer, are substantial and demand an understanding at a molecular level. New approaches to treatment could be revealed by dissecting the molecular pathways that control sexually dimorphic phenotypes. Sexual differentiation is in large part an epigenetic phenomenon and hence studying disparities in threshold for transformation in male and female cells that are syngeneic except in their sex chromosomes, provides a powerful tool to investigate epigenetic mechanisms that establish this dimorphic tumorigenic phenotype. To address these important questions, we utilized our GBM model in which male and female cells exhibit markedly different sensitivities to transformation upon loss of neurofibromin and p53 function and activation of the EGF receptor pathway (12). We have previously demonstrated transcriptome-wide differences in gene expression and clonogenic stem cell function in these male and female GBM cells (11, 12) and therefore we

hypothesized that these differences are endowed by sex-specific epigenetic mechanisms and more specifically sex-specific Brd4-bound enhancer activity.

Brd4 is an epigenetic reader that binds acetylated histones H3 and H4 throughout the entire cell cycle and is known to be deregulated in numerous cancers (30). Brd4 is thought to play a central role in cancer by promoting epithelial-to-mesenchymal transition, stem cell-like conversion, and pluripotency (19, 20, 31), and the pharmacological inhibition of this protein has shown therapeutic activity in a number of different cancer models (28, 32-35). Additionally, Brd4-bound enhancers have been shown to play key roles in establishing cell identity. We therefore mapped Brd4 genomic localization in male and female GBM cells and revealed that approximately 13% of Brd4-bound enhancers are sex-specific, with 87% shared between the two sexes. Next, we demonstrated that approximately 81% of these Brd4-bound enhancers were also enriched for H3K27ac indicative of sex-specific highly active enhancer regions. Thus, for the first time, sex is established as an intrinsic element of cellular identity that is driven by Brd4 activity. To further validate whether the phenotypic differences in male and female GBM cells are indeed mediated by Brd4, as was suggested by our transcriptome-wide gene expression and Brd4 binding analyses, we performed Brd4 knockdown using shRNA in male and female GBM cells to examine if we can reverse these differences upon depletion of Brd4 function. Interestingly, Brd4 depletion decreased clonogenic stem cell frequency in male cells while increasing it in female cells abrogating the sex differences observed in the tumorigenic phenotype. These exciting results suggest that differential sex-specific Brd4 localization may be responsible for the sex differences in GBM. Additionally, and given that Brd4 is shown to have pleiotropic functions in the regulation of gene expression, these results

suggest that Brd4 can exhibit dual functions in GBM as an oncogene or a tumor suppressor dependent upon cellular sex.

Importantly, as bromodomain inhibitors are currently being evaluated in clinical trials, we tested the effect of a panel of clinically available BET_is on the tumorigenic phenotype in male and female GBM cells. We found that male and female murine and human GBM cells responded in diametrically opposed ways to BET inhibition. Consistent with our knockdown data, this dimorphism in Brd4 function is linked to the sex of the experimental cells and is correlated with sex-specific patterns of Brd4 localization throughout the genome, which renders male and female cells differentially sensitive to BET_i treatment. Accordingly, BET inhibition with the two most potent inhibitors in male and female GBM cells, JQ1 and CPI0610 respectively, decreased growth of male *in vivo* tumors but increased growth of female tumors. These results strongly indicate that sex differences in disease biology translate into sex differences in therapeutic responses. Although the discrepancy in the magnitude of the effect of the two BET_is on the *in vivo* tumorigenic phenotype could not be explained by the actions of other Brd family members, both drugs show a sex-specific effect that diminished the basal sex differences in tumor phenotypes. The opposing sex-specific response to the inhibition of Brd4 in our GBM model could explain the previously published data in breast and prostate cancer, wherein ectopic expression of Brd4 in breast cancer cells decreased invasiveness and tumor growth, while Brd4 inhibition decreased viability of prostate cancer cells (34, 47, 48). These studies also revealed, that in women with estrogen receptor positive breast cancer (47) or endometrial cancer (48), low Brd4 expression is correlated with worsened survival. This is in contrast to men with prostate cancer, in whom low levels of Brd4 are associated with improved survival (34, 48).

Finally, the functions of Brd4 are determined by the action of master transcriptional regulators that bind directly or indirectly to Brd4 and dictate its localization in the genome. We performed a motif-based analysis to identify potential transcription factors that endow Brd4 with its pro- or anti-tumorigenic functions. This analysis revealed that Brd4 co-localizes in a sex-specific manner with Myc and p53 in male and female GBM cells, respectively. These exciting preliminary results warrant further functional studies to validate whether these master transcription factors drive the sex differences in Brd4-bound enhancer activity (sex-specific Brd4 genomic localization) and therefore the sex differences in tumorigenic phenotype and response to BET inhibitor treatment.

Altogether, the consistency between our mouse and human data, the GBM TCGA data, and published breast and prostate cancer studies, provides strong evidence for the context-dependent, sex-specific dual role of Brd4 in regulating gene expression programs in oncogenesis. In future work, we will take advantage of this remarkable dimorphism in Brd4 function in glioblastoma to better define the molecular basis for Brd4 pleiotropy in cancer and mechanisms of resistance to Brd4 inhibitors. Since bromodomain inhibitors are currently being evaluated in a number of clinical trials, understanding this phenomenon is of critical importance, both for the interpretation of existing trials and to guide better application of these drugs. Increasing our knowledge of these sex-specific genetic and epigenetic mechanisms will lead to a greater understanding of cancer biology and its relationship to normal development. Importantly, we have identified sex-specific Brd4-regulated genes and pathways, which could translate into new and promising therapeutic targets to enhance survival for all GBM patients and potentially other cancers that exhibit substantial sex differences in incidence or outcome.

Materials and Methods

Transposon calling cards assay for Brd4 binding

For each sample (female and male murine GBM cells), 10 wells with an area of 9.5 mm^2 were seeded at 50% confluency (200,000 cells per well of a 6-well plate). Each well represented a unique set of insertion events and was processed individually. Briefly, each well received 3 µg of plasmid DNA containing a *piggyBac* transposon (carrying a puromycin selection marker) with or without 3 µg of a transposase plasmid encoding Brd4 fused to the N-terminus of hyperactive *piggyBac* (HyPBase). Plasmids were delivered using Lipofectamine LTX/Plus Reagent (Invitrogen). Before transfection, cells were incubated in DMEM without FBS or antibiotics for 30 minutes, and then replaced with fresh media containing DMEM/F12 with 10% FBS and 1% penicillin-streptomycin. Transfection complexes were applied to cells for 12-18 hours at 37 °C and 5% CO_2. Cells were allowed to recover in fresh medium for another 24-48 hours. Each well was then separately expanded onto 10 cm dishes and placed in medium containing puromycin at a concentration of 2.5 µg/ml for 3 days. After 3 days, cells that received transposon DNA alone showed no growth, while those that also received transposase DNA showed robust growth. Each 10 cm dish of expanded puromycin resistant cells were harvested and processed by a modified version of the transposon calling card protocol as previously described (37). The Calling Card library was prepared by assigning each well a unique Illumina P7 index, so that each well of a sample could be demultiplexed as a set of unique barcoded insertions. All 4 sets of libraries, (Male_PB_helper, Male_PB_Brd4_fusion, Female_PB_helper, and Female_PB_Brd4_fusion) were then pooled and sequenced on an Illumina HiSeq 300. A total of 40 Illumina P7 indexes were demultiplexed (10 replicates per library). Reads were mapped to the mm10 reference genome using Novoalign

(version 3.08.02; Novocraft Technologies SDN BHD). For each library, data from constituent replicates were pooled and discrete insertions exported in Calling Card library format for subsequent analysis. Insertions were visualized on the WashU Epigenome Browser (v46.1).

Chromatin immunoprecipitation sequencing (ChIP-seq) for H3K27ac

10 million male and female GBM cells were treated with 0.05% DMSO or 500 nM JQ1 for 24 hours. Following treatment, cells were then prepared for various downstream analyses including ChIP-seq for H3K27ac. Briefly, cells were fixed in 1% formaldehyde prepared in DMEM/F12 and incubated for 10 minutes at room temperature with gentle rocking. Fixation was quenched by the addition of glycine to a final concentration of 125 mM and incubation for 10 minutes at room temperature with gentle rocking. Cells were then washed with cold PBS and harvested by scraping in 5 ml of cold PBS. Cells were transferred to 15 mL conical tubes and pelleted with a 5-minute spin (1,000g) at 4ºC. Sonication was performed on an Epishear probe-in sonicator (Active Motif) at 40% amplitude for 8 cycles of 30 seconds with 30 seconds of rest between each cycle. ChIP-seq libraries were constructed as previously described (49), with an antibody that recognizes H3K27Ac (Active Motif, 39133, rabbit polyclonal). ChIP-seq libraries were constructed with sample-specific barcodes, and pooled before sequencing on a HiSeq 2500 (Illumina).

RNA-sequencing

Male and female GBM cells (Nf1-/-;DNp53 astrocytes) were generated as previously reported (Sun et al., 2015) and grown in DMEM/F12 media supplemented with 10% FBS and 1% penicillin-streptomycin. Total RNA was isolated from male and female GBM cells that were treated with DMSO (0.05%) or JQ1 (500 nM for 24 hours) using the RNeasy Mini Kit from QIAGEN (Hilden,

Germany), following the kit protocol. PolyA Selection was performed to create RNA Seq libraries. Cell mRNA was extracted from total RNA using a Dynal mRNA Direct kit. The quantity of RNA was measured using a spectrophotometer (NanoDrop 2000c; Thermo Scientific). Samples with an RNA concentration A260/A280 ≥1.8 ng/µl, and purity A230/A260 ≥ 2.0 ng/µl were selected. The Agilent 2100 Bioanalyzer was used to determine the RNA integrity number. The degradation level was identified using the RNA 6000 Nano LabChip kit (Agilent). Samples with RNA integrity number > 9.8 were further processed using TruSeq mRNA Library Preparation Kit (Illumina) and then sequenced on a HiSeq 25000 (Illumina).

Sequencing data alignment and analysis

Raw reads from transposon calling cards were aligned to the murine genome build mm10 using Bowtie2 (50). Significant Calling Cards peaks or Brd4 enriched enhancer sites were identified by a modified version of the previously described algorithm, which also has similarities to the MACS2 ChIP-Seq peak caller (37). Briefly, transposon insertions were grouped into peaks using a hierarchical clustering algorithm with a maximum distance of 5 Kb between insertions. Significant peaks were identified using Poisson distribution to test for enrichment over the background (unfused transposase) Calling Card data. The expected number of hops per TTAA was estimated by considering the total number of insertions observed in a large region of 100 Kb distance centered at the Calling Card cluster. We computed a *p*-value based on the expected number of insertions and identified Brd4 enriched enhancer sites with *p*-values <0.05.

To identify the sites with an excess of Brd4 insertions in male GBM cells relative to female cells, we used the algorithm from ChIP-Seq peaks caller MACS (51) but modified for the analysis of calling card data. First, the Brd4-enriched enhancer sites from both male and female cells were

merged if they overlapped by more than 1bp. For each merged or unmerged enhancer site, the insertions from the female samples were used to compute the lambda of Poisson distribution. We then computed a *p*-value from cumulative distribution function of the observed number of independent insertions in the male sample. Brd4 binding sites with *a p*-value less than 0.05 were considered as Brd4 binding sites significantly enriched in male sample. To identify the Brd4 sites with an excess of insertions in female GBM cells relative to male cells, we performed the same analysis, substituting the male and female data sets.

ChIP-seq data sets for H3K27ac were aligned to the murine genome build mm10 using Bowtie2 and only uniquely aligning reads were used (50). Regions of enrichment of H3K27ac over background were calculated using the MACS version (2.1.0) peak finding algorithm (51). An adjusted *p*-value threshold of enrichment of 0.01 was used for all data sets. The resulting peak files were used as inputs for DiffBind (version 3.5) to derive consensus peak sets (52, 53). The differential enrichment of H3K7Ac signals between male and female analysis was carried out with Diffbind using DESeq2 (method = DBA_DESEQ2) with libraries normalized to total library size.

RNA-seq data sets were aligned to the transcriptome and the whole-genome with STAR (54). Genes or exons were filtered for just those that were expressed. A gene count table for all the genes in each sample was generated using HTSeq (55). Differential gene expression between pairs of samples was computed using DESeq2 and was filtered by FDR < 0.05 for differentially expressed genes (56).

Pathway analysis

Pathway enrichment analysis for differentially regulated genes was performed using a combination of KEGG pathway and Genomatix Pathway System (GePS). GePS uses information extracted

from public and proprietary databases to display canonical pathways and or to create and extend networks based on literature data. These sources include NCI-Nature Pathway Interaction Database, Biocarta, Reactome, Cancer Cell Map, and the ENCODE Transcription Factor project data. All data for pathway analyses are presented with adjusted corrected *p*-values.

shRNA lentiviral infection and knockdown of Brd2, Brd3 and Brd4

Brd2, Brd3 and Brd4 knockdown lines were generated by infecting male and female GBM cells (Nf1-/-;DNp53 astrocytes) with lentiviral shRNAs against Brd2, Brd3 or Brd4. All Knockdown lines were selected with puromycin (2.5 μg/ml) in media for 1-2 weeks and the survivors were expanded for downstream target knockout analysis. Five different shRNAs specific to each of the Brd family members were evaluated and the shRNA with the most robust knockdown was used for the downstream functional experiments. Sequences for shRNAs are provided in **Supplementary Table 3**.

Quantitative Real-Time PCR

Total RNA was isolated using QIAGEN RNeasy Mini Kit from male and female GBM cells (Nf1-/-;DNp53 astrocytes) infected with shRNA lentivirus against Brd2, Brd3 or Brd4. cDNA was generated using the QuantiTect Reverse Transcription Kit (Qiagen). Quantitative RT-PCR was performed using gene-specific primers and iTaq SYBR Green PCR master mix (Biorad, CA). Data was analyzed by standard ΔCq method (2-ΔΔCq) where ΔCq is the difference between the gene of interest and GAPDH control Cq value. Sequences for primers specific for each Brd family member are provided in **Supplementary Table 3**.

Clonogenic cell frequency assay: Extreme Limiting Dilution Assays (ELDA analysis)

Male and female mouse GBM cells (Nf1-/-;DNp53 astrocytes, 2 lots of male and female cells) or human male and female primary GBM cell lines (3 male and 3 female human primary GBM cell lines were kindly provided to us by Dr. Albert Kim) were treated with DMSO (0.05%), iBET762 (4μM), CPI203 (0.5μM), CPI0610 (1μM), JQ1 (500 nM), OTX015 (2.5μM), PFI1 (5μM) or RVX-208 (5μM) for 24 hours or with shRNAs against Brd2, Brd3, or Brd4. Clonogenic capacity was then assessed by the Extreme Limiting Dilution Assay (ELDA). The frequency of clonogenic stem cells was evaluated by the cells' ability to form tumor-sphere in low-adherent conditions as previously reported (12). Briefly, cells were harvested into a single cell suspension and plated in neurosphere media containing EGF, FGF and mouse LIF on 96-well ultra-low attachment plates in a serial dilution ranging from 3000 cells/well to 1 cell/well (3000, 600, 120, 24, 5 and 1 cells; n=14-18 wells/cell density). Sphere formation was measured 7 days after plating. Clonogenic cell frequency was then analyzed using the Extreme Limiting Dilution Analysis software.

***In vivo* tumorigenesis: flank implantation**

Flank tumors were generated by implanting GBM astrocytes at various cell numbers subcutaneously into left side flanks. These cells were treated with 0.05% DMSO, 500 nM JQ1 or 1 μM CPI0610 for 24 hours followed by EGF treatment at 50ng/ml for one week. 1.5 million female cells or 5000 male cells treated with DMSO, JQ1 or CPI0610 were then harvested and resuspended in 100 μl of 1:1 media to matrigel (BD Biosciences) and injected into the flanks of mice. Mice were monitored weekly and tumor growth was monitored blindly for 12 weeks with thrice weekly micrometer measurements in 3 dimensions. Animals were used in accordance with an animal studies protocol (no. 20180206) approved by the Animal Studies Committee of the

Washington University School of Medicine per the recommendations of the Guide for the Care and Use of Laboratory Animals (NIH).

Bioinformatic motif analysis

To identify DNA motifs that are associated with sex-specific Brd4 binding we used the HOMER toolkit (57). Briefly, to find motifs enriched under male-specific peaks, we used the sequences under male-specific Brd4 peaks as input to HOMER, and used sequences from female-specific peaks, or all Brd4 peaks, as background. we used the following HOMER command: (findMotifsGenome.pl mm10 -nomotif -preparsedDir -bg). We found motifs enriched under female-specific peaks in a similar fashion using the corresponding sequence files.

TCGA gene expression data analysis

RNA-seq expression data for TCGA GBM samples were obtained from the Broad GDAC Firehose data portal. Clinicopathologic and genomic data for the GBM samples were obtained from the cBioPortal for cancer genomics (46). To investigate whether the concordance of expression of sex-specific Brd4-bound, H3K27ac enriched genes with differential gene expression in male and female GBM mouse cells and human GBM samples could be due to random chance, we calculated *p*-values using the cumulative hypergeometric distribution and found that the probability of observing a 23.2% and 14.3% concordance in male and female data sets had a *p*-value of 0.045 and 0.016 in male and female data sets, respectively.

Statistical analysis

All experiments in this study were carried out at least three times. ELDA experiments with JQ1 and CPI0610 treatment were performed three times (n=3) in three different mouse GBM lots of cells (n=3). ANOVA, two-tailed Student's t-test and Fisher's exact test were used to compare the differences in all functional measurements between BET inhibitors and control group (DMSO), and a p-value < 0.05 was considered statistically significant.

To test if upregulated genes in male cells compared to female cells and vice versa are significantly enriched for H3K27ac binding, the normalized H3K27ac signal intensities (reads) from 1kb upstream of the gene start site to 1kb downstream of the end of the gene were used for the correlation analysis. A paired Mann-Whitney-Wilcoxon test was used to compare normalized H3K27ac signal intensities between male and female cells and a p-value less than 0.01 was considered statistically significant.

To investigate if Brd4-proximal genes are significantly downregulated upon JQ1 treatment compared to Brd4-distal genes, we first defined Brd4 proximal genes as the closest genes to Brd4 binding sites and Brd4 distal genes as genes located near sites that are not enriched for Brd4 binding sites. Brd4 proximal and distal genes (500 genes each) were randomly selected. A Mann-Whitney-Wilcoxon test was used to compare the expression profiles before and after JQ1 treatment of Brd4 proximal and distal genes for male and female respectively and a p-value less than 0.01 was considered statistically significant.

Data and materials availability: All Illumina sequencing reads and processed file have been deposited in the Short Read Archive/GEO database (http://www.ncbi.nlm.nih.gov/geo/).

References:

1. Ober C, Loisel DA, & Gilad Y (2008) Sex-specific genetic architecture of human disease. *Nat Rev Genet* 9(12):911-922.
2. Ostrom QT*, et al.* (2014) The epidemiology of glioma in adults: a "state of the science" review. *Neuro Oncol* 16(7):896-913.
3. Ang C, Guiot MC, Ramanakumar AV, Roberge D, & Kavan P (2010) Clinical significance of molecular biomarkers in glioblastoma. *Can J Neurol Sci* 37(5):625-630.
4. Ostrom QT*, et al.* (2016) CBTRUS Statistical Report: Primary Brain and Other Central Nervous System Tumors Diagnosed in the United States in 2009-2013. *Neuro Oncol* 18(suppl_5):v1-v75.
5. Siegel R*, et al.* (2012) Cancer treatment and survivorship statistics, 2012. *CA Cancer J Clin* 62(4):220-241.
6. Siegel R, Naishadham D, & Jemal A (2012) Cancer statistics for Hispanics/Latinos, 2012. *CA Cancer J Clin* 62(5):283-298.
7. Sun T, Warrington NM, & Rubin JB (2012) Why does Jack, and not Jill, break his crown? Sex disparity in brain tumors. *Biol Sex Differ* 3:3.
8. Koehler JW*, et al.* (2018) A Revised Diagnostic Classification of Canine Glioma: Towards Validation of the Canine Glioma Patient as a Naturally Occurring Preclinical Model for Human Glioma. *J Neuropathol Exp Neurol* 77(11):1039-1054.
9. Ostrom QT, Rubin JB, Lathia JD, Berens ME, & Barnholtz-Sloan JS (2018) Females have the survival advantage in glioblastoma. *Neuro Oncol* 20(4):576-577.

10. Dorak MT & Karpuzoglu E (2012) Gender differences in cancer susceptibility: an inadequately addressed issue. *Front Genet* 3:268.

11. Kfoury N*, et al.* (2018) Cooperative p16 and p21 action protects female astrocytes from transformation. *Acta Neuropathol Commun* 6(1):12.

12. Sun T*, et al.* (2014) Sexually dimorphic RB inactivation underlies mesenchymal glioblastoma prevalence in males. *J Clin Invest* 124(9):4123-4133.

13. Yang W*, et al.* (2019) Sex differences in GBM revealed by analysis of patient imaging, transcriptome, and survival data. *Sci Transl Med* 11(473).

14. Nugent BM & McCarthy MM (2011) Epigenetic underpinnings of developmental sex differences in the brain. *Neuroendocrinology* 93(3):150-158.

15. McCarthy MM & Nugent BM (2015) At the frontier of epigenetics of brain sex differences. *Front Behav Neurosci* 9:221.

16. Belkina AC & Denis GV (2012) BET domain co-regulators in obesity, inflammation and cancer. *Nature reviews. Cancer* 12(7):465-477.

17. Berenguer-Daize C*, et al.* (2016) OTX015 (MK-8628), a novel BET inhibitor, displays in vitro and in vivo antitumor effects alone and in combination with conventional therapies in glioblastoma models. *Int J Cancer* 139(9):2047-2055.

18. Pastori C*, et al.* (2014) BET bromodomain proteins are required for glioblastoma cell proliferation. *Epigenetics* 9(4):611-620.

19. Wu T & Donohoe ME (2015) The converging roles of BRD4 and gene transcription in pluripotency and oncogenesis. *RNA & disease* 2(3).

20. Wu T, Pinto HB, Kamikawa YF, & Donohoe ME (2015) The BET family member BRD4 interacts with OCT4 and regulates pluripotency gene expression. *Stem cell reports* 4(3):390-403.

21. Xu L*, et al.* (2018) Targetable BET proteins- and E2F1-dependent transcriptional program maintains the malignancy of glioblastoma. *Proceedings of the National Academy of Sciences of the United States of America* 115(22):E5086-E5095.

22. Dowen JM*, et al.* (2014) Control of cell identity genes occurs in insulated neighborhoods in mammalian chromosomes. *Cell* 159(2):374-387.

23. Hnisz D*, et al.* (2013) Super-enhancers in the control of cell identity and disease. *Cell* 155(4):934-947.

24. Hnisz D*, et al.* (2015) Convergence of developmental and oncogenic signaling pathways at transcriptional super-enhancers. *Mol Cell* 58(2):362-370.

25. Ounzain S & Pedrazzini T (2016) Super-enhancer lncs to cardiovascular development and disease. *Biochim Biophys Acta* 1863(7 Pt B):1953-1960.

26. Parker SC*, et al.* (2013) Chromatin stretch enhancer states drive cell-specific gene regulation and harbor human disease risk variants. *Proceedings of the National Academy of Sciences of the United States of America* 110(44):17921-17926.

27. Whyte WA*, et al.* (2013) Master transcription factors and mediator establish super-enhancers at key cell identity genes. *Cell* 153(2):307-319.

28. Filippakopoulos P*, et al.* (2010) Selective inhibition of BET bromodomains. *Nature* 468(7327):1067-1073.

29. Liu Z*, et al.* (2017) Drug Discovery Targeting Bromodomain-Containing Protein 4. *J Med Chem* 60(11):4533-4558.

30. Filippakopoulos P & Knapp S (2014) Targeting bromodomains: epigenetic readers of lysine acetylation. *Nature reviews. Drug discovery* 13(5):337-356.

31. Alsarraj J*, et al.* (2011) Deletion of the proline-rich region of the murine metastasis susceptibility gene Brd4 promotes epithelial-to-mesenchymal transition- and stem cell-like conversion. *Cancer research* 71(8):3121-3131.

32. Delmore JE*, et al.* (2011) BET bromodomain inhibition as a therapeutic strategy to target c-Myc. *Cell* 146(6):904-917.

33. Loven J*, et al.* (2013) Selective inhibition of tumor oncogenes by disruption of super-enhancers. *Cell* 153(2):320-334.

34. Urbanucci A*, et al.* (2017) Androgen Receptor Deregulation Drives Bromodomain-Mediated Chromatin Alterations in Prostate Cancer. *Cell reports* 19(10):2045-2059.

35. Ali I, Choi G, & Lee K (2017) BET Inhibitors as Anticancer Agents: A Patent Review. *Recent Pat Anticancer Drug Discov*.

36. Wang H, Mayhew D, Chen X, Johnston M, & Mitra RD (2011) Calling Cards enable multiplexed identification of the genomic targets of DNA-binding proteins. *Genome Res* 21(5):748-755.

37. Wang H, Mayhew D, Chen X, Johnston M, & Mitra RD (2012) "Calling cards" for DNA-binding proteins in mammalian cells. *Genetics* 190(3):941-949.

38. Heintzman ND*, et al.* (2009) Histone modifications at human enhancers reflect global cell-type-specific gene expression. *Nature* 459(7243):108-112.

39. Yamaguchi T, Hosono Y, Yanagisawa K, & Takahashi T (2013) NKX2-1/TTF-1: an enigmatic oncogene that functions as a double-edged sword for cancer cell survival and progression. *Cancer Cell* 23(6):718-723.

40. Caswell DR, *et al.* (2018) Tumor Suppressor Activity of Selenbp1, a Direct Nkx2-1 Target, in Lung Adenocarcinoma. *Mol Cancer Res*.

41. Han W, *et al.* (2018) ZIC1 acts a tumor suppressor in breast cancer by targeting survivin. *Int J Oncol* 53(3):937-948.

42. Qiang W, *et al.* (2014) ZIC1 is a putative tumor suppressor in thyroid cancer by modulating major signaling pathways and transcription factor FOXO3a. *J Clin Endocrinol Metab* 99(7):E1163-1172.

43. Najafova Z, *et al.* (2017) BRD4 localization to lineage-specific enhancers is associated with a distinct transcription factor repertoire. *Nucleic acids research* 45(1):127-141.

44. Daniel B, Nagy G, & Nagy L (2014) The intriguing complexities of mammalian gene regulation: how to link enhancers to regulated genes. Are we there yet? *FEBS Lett* 588(15):2379-2391.

45. Bhagwat AS, *et al.* (2016) BET Bromodomain Inhibition Releases the Mediator Complex from Select cis-Regulatory Elements. *Cell reports* 15(3):519-530.

46. Cerami E, *et al.* (2012) The cBio cancer genomics portal: an open platform for exploring multidimensional cancer genomics data. *Cancer Discov* 2(5):401-404.

47. Crawford NP, *et al.* (2008) Bromodomain 4 activation predicts breast cancer survival. *Proceedings of the National Academy of Sciences of the United States of America* 105(17):6380-6385.

48. Janouskova H, *et al.* (2017) Opposing effects of cancer-type-specific SPOP mutants on BET protein degradation and sensitivity to BET inhibitors. *Nat Med* 23(9):1046-1054.

49. Reddy TE, *et al.* (2009) Genomic determination of the glucocorticoid response reveals unexpected mechanisms of gene regulation. *Genome Res* 19(12):2163-2171.

50. Langmead B & Salzberg SL (2012) Fast gapped-read alignment with Bowtie 2. *Nat Methods* 9(4):357-359.

51. Zhang Y*, et al.* (2008) Model-based analysis of ChIP-Seq (MACS). *Genome Biol* 9(9):R137.

52. Ross-Innes CS*, et al.* (2012) Differential oestrogen receptor binding is associated with clinical outcome in breast cancer. *Nature* 481(7381):389-393.

53. Stark RaB, G. (2011) DiffBind: differential binding analysis of ChIP-Seq peak data.

54. Dobin A*, et al.* (2013) STAR: ultrafast universal RNA-seq aligner. *Bioinformatics* 29(1):15-21.

55. Anders S, Pyl PT, & Huber W (2015) HTSeq--a Python framework to work with high-throughput sequencing data. *Bioinformatics* 31(2):166-169.

56. Love MI, Huber W, & Anders S (2014) Moderated estimation of fold change and dispersion for RNA-seq data with DESeq2. *Genome Biol* 15(12):550.

57. Heinz S*, et al.* (2010) Simple combinations of lineage-determining transcription factors prime cis-regulatory elements required for macrophage and B cell identities. *Mol Cell* 38(4):576-589.

Acknowledgments: This work was supported by NIH RO1 CA174737 (JBR), R01 NS076993 (RM), R21 HG009750 (RM), U01 MH109133 (RM), RF1 MH117070 (RM), Joshua's Great Things (JBR), The Children's Discovery Institute (JBR and RM) and NIH T32GM007200, T32HG000045, and F30HG009986 (AM). We thank the Genome Technology Access Center in the Department of Genetics at Washington University School of Medicine for help with genomic analysis. The Center is partially supported by NCI Cancer Center Support Grant #P30 CA91842

to the Siteman Cancer Center and by ICTS/CTSA Grant# UL1 TR000448 from the National Center for Research Resources (NCRR), a component of the National Institutes of Health (NIH), and NIH Roadmap for Medical Research. This publication is solely the responsibility of the authors and does not necessarily represent the official view of NCRR or NIH.

Author contributions: NK and ZQ designed and performed experiments, analyzed data and wrote the manuscript. MW and AM developed and optimized the calling cards protocol. MW and XC performed the calling card experiments and generated libraries. LB provided significant edits to the manuscript and suggestions to the experiments and data analyses as well as blindly analyzed ELDA experiments. AM developed the software to analyze and visualize calling card data. KB and JG performed ChIP-seq experiments. SS assisted in the RNA-seq analysis. JBR and RM designed experiments, analyzed data, edited the manuscript and supervised the project. All authors read and approved the final version of the manuscript.

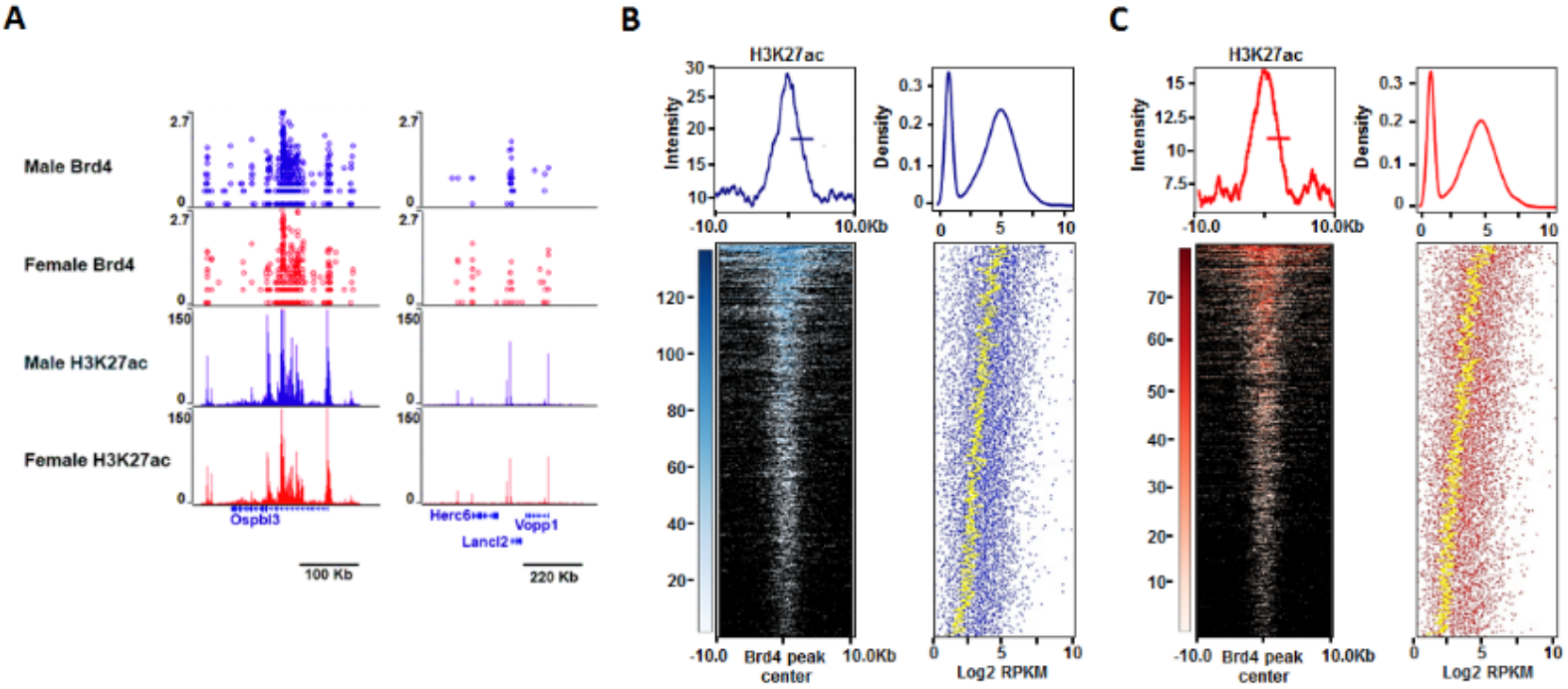

Figure 1. Concordance between Brd4-bound enhancers, H3K27ac enrichment, and gene expression in mouse GBM astrocytes. (A) A representative example of concordant Brd4 and H3K27ac binding at high and low-enriched regions in male and female GBM astrocytes. **(B-C)** Heatmaps and intensity plots of H3K27ac signal at sex-specific Brd4-enriched peaks (+/- 10 Kb from the Brd4 peak center) in male **(B)** and female **(C)** GBM cells. For each sex-specific Brd4-enriched peak, the expression values of the nearest gene are presented in a dot plot in which the yellow-dotted line depicts the average gene expression levels of 50 genes (Density refers to the number of genes). These analyses revealed that Brd4 binding sites are significantly enriched at H3K27ac candidate enhancer regions and display concordant gene expression levels indicative of active Brd4-bound enhancers ($p < 0.01$).

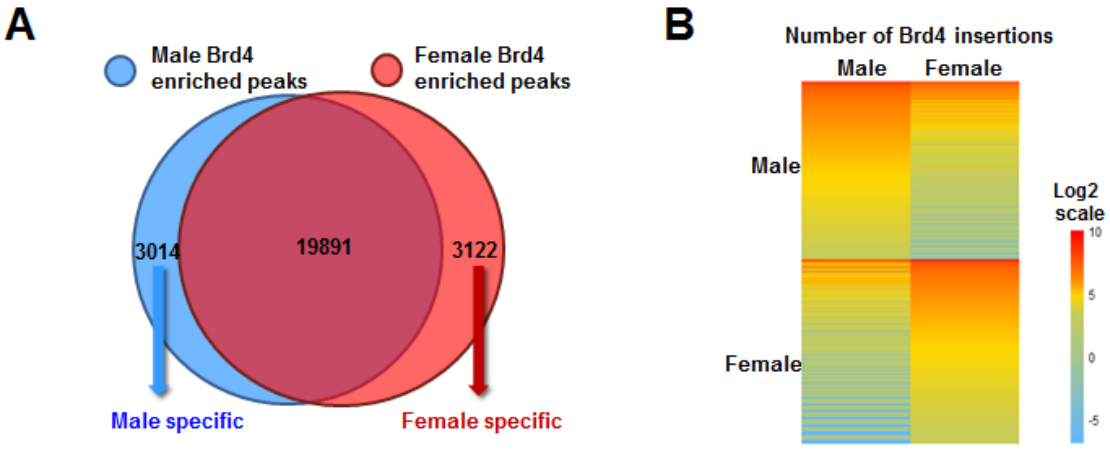

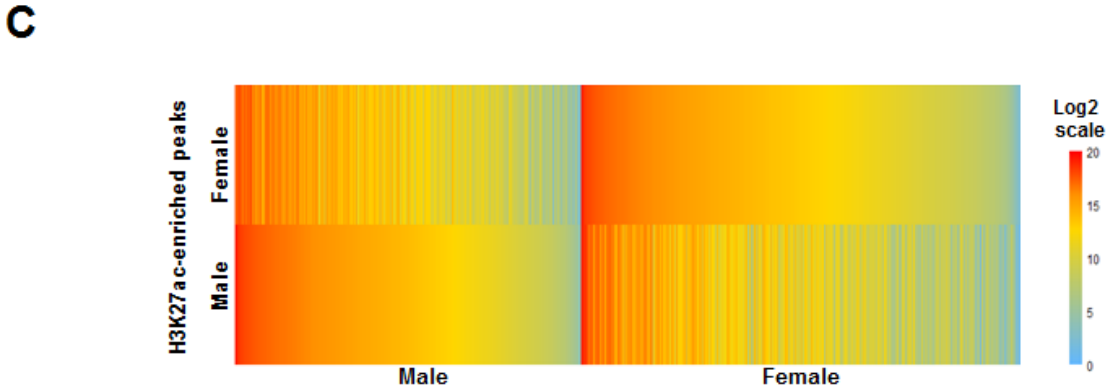

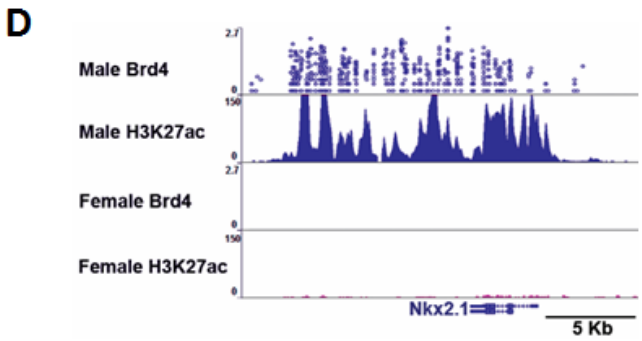

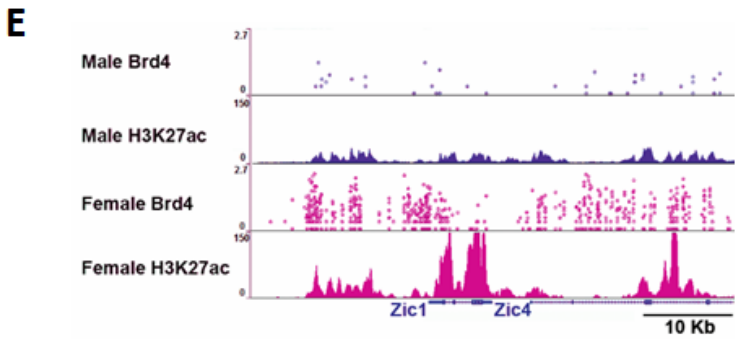

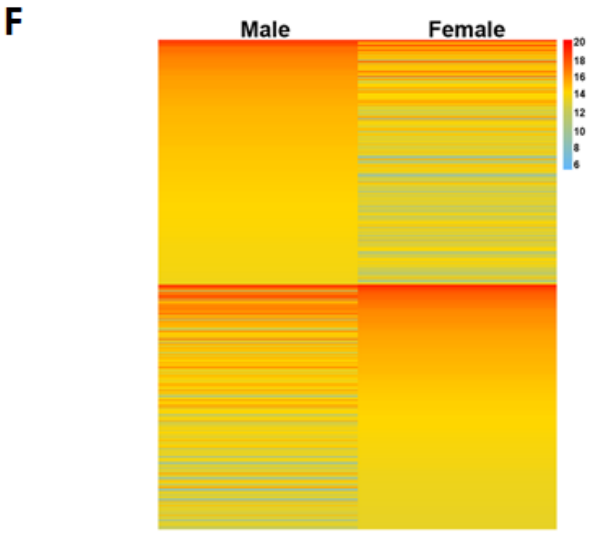

G

Pathway enrichment analysis for differentially regulated sex-specific Brd4-bound genes in male and female GBM cells*

Pathway description	Adjusted *p*-value	# of Genes
Metabolic process	0.00E+00	568
Chromosome aberrations	0.00E+00	523
Cell differentiation	0.00E+00	348
Glioblastoma	0.00E+00	281
Cell proliferation	0.00E+00	181
Cell migration	0.00E+00	160
Cell death	0.00E+00	159
DNA binding-Transcription factors	0.00E+00	90
TGF beta signaling	0.00E+00	87
Stem cells (differentiation, proliferation)	0.00E+00	77
Cell invasion	0.00E+00	73
Tumor angiogenesis	0.00E+00	70
Integrin signaling	4.00E-03	31
Semaphorin signaling	1.20E-02	16

*Subset of pathway enrichment analysis

Figure 2. Male and female GBM cells have sexually dimorphic Brd4-bound enhancers. (A) Venn-diagram showing the number of unique male (3014), unique female (3122), and overlapping (19,891) Brd4-enriched peaks identified in GBM astrocytes. **(B)** A heatmap depiction of the number of Brd4 insertions at male and female-specific Brd4-enriched peaks in GBM astrocytes (normalized data). **(C)** A heatmap analysis of H3K27ac signal intensity (read depth) at male and female-specific Brd4-enriched peaks in GBM astrocytes. **(D)** Nkx2.1 and **(E)** Zic1/4 illustrate male and female-specific genes, respectively, associated with differential Brd4 binding affinity and H3K27ac enrichment. The x-axis (blue arrows) of all tracks corresponds to genomic location of the gene. The y-axis of Calling Card tracks represents the log10 scale of sequencing reads for each insertion as indicated by circles. The y-axis of ChIP-seq tracks represents the number of uniquely mapped reads. **(F)** RNA abundance (RNA sequencing) in male and female GBM cells for differentially regulated sex-specific Brd4-bound genes (n=3)). **(G)** Pathway enrichment analysis for differentially regulated sex-specific Brd4-bound genes in male and female GBM astrocytes.

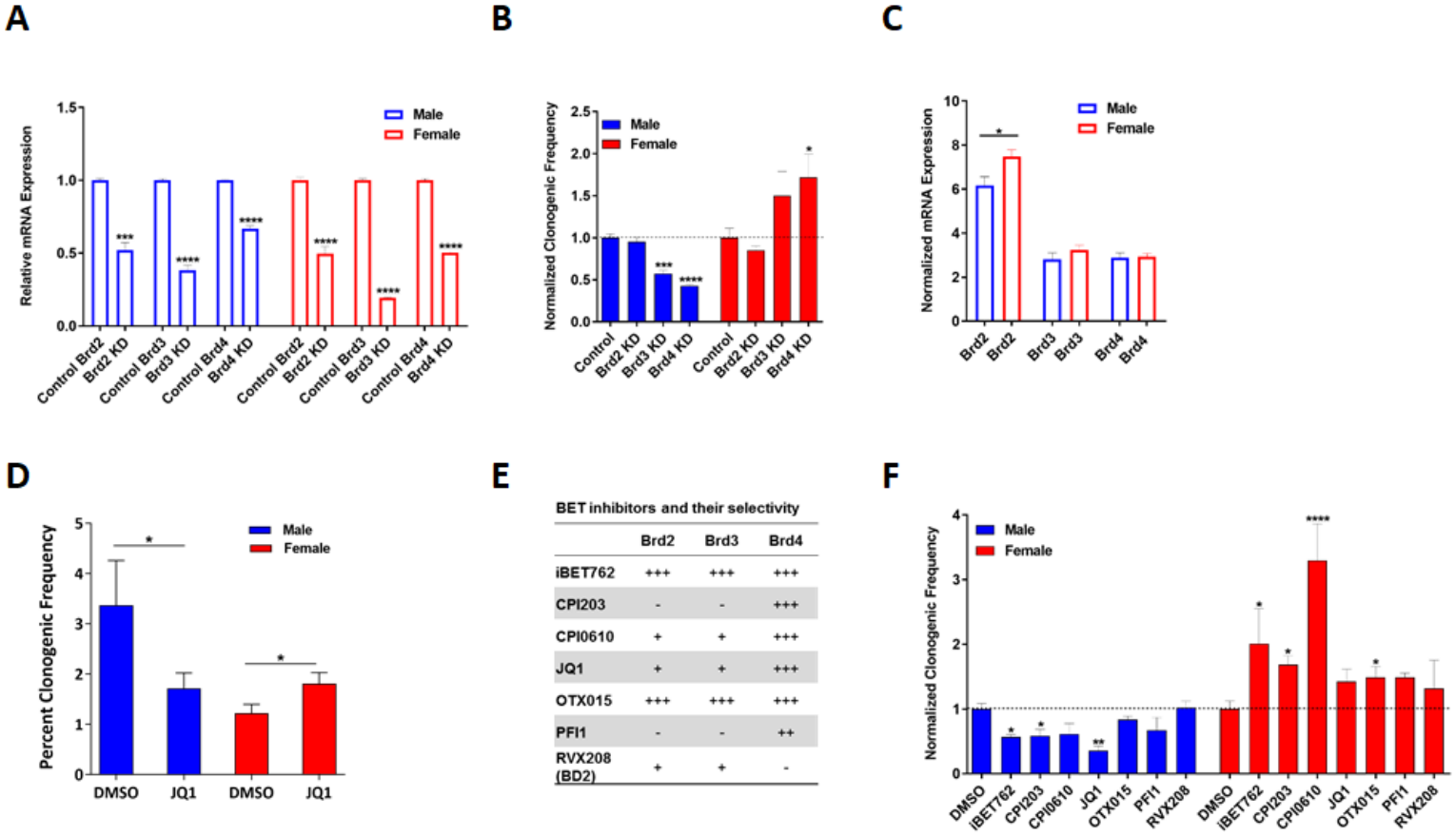

Figure 3. Brd4 inhibition has opposing effects on clonogenicity in male and female GBM astrocytes. (A) Brd2, Brd3, and Brd4 mRNA expression following lentiviral shRNA infection. mRNA levels in knockdown samples were normalized to their respective control. **(B)** Normalized clonogenic cell frequency as determined by ELDA assay in control and Brd2, Brd3, and Brd4 knockdown male and female GBM cell lines. Knockdown of Brd4 and Brd3 suppresses clonogenic frequency in male GBM cells while female cells showed a significant increase in clonogenic frequency following Brd4 knockdown only. Brd2 depletion was without effect. All treatment groups were normalized to control clonogenic frequency levels. **(C)** Normalized Brd2, Brd3 and Brd4 mRNA expression in male and female GBM cells under basal conditions. Brd3 and Brd4 are expressed at equivalent levels between male and female GBM cells, while Brd2 is expressed at higher levels in female cells. **(D)** Percent clonogenic cell frequency as determined by ELDA assay in male and female GBM cells treated with DMSO or JQ1. Male cells exhibited greater clonogenic cell activity than female cells under control conditions. JQ1 significantly reduced clonogenic cell frequency in male cells to levels almost equivalent to female cells under control conditions, while female cells exhibited a significant increase in their clonogenic cell frequency. **(E)** Tabular representation of the BET inhibitors currently in clinical trials and their selectivity to the three BET family members. **(F)** Normalized clonogenic cell frequency as determined by ELDA assay in male and female GBM cells treated with DMSO (control) or the indicated BET inhibitor. BET inhibitors significantly reduced clonogenic cell frequency in male cells, and significantly increased clonogenic cell frequency in female cells. (*=p <0.05, **=p <0.01, ***=p <0.001, ****=p <0.0001 as determined by two-tailed t-test or one-way ANOVA).

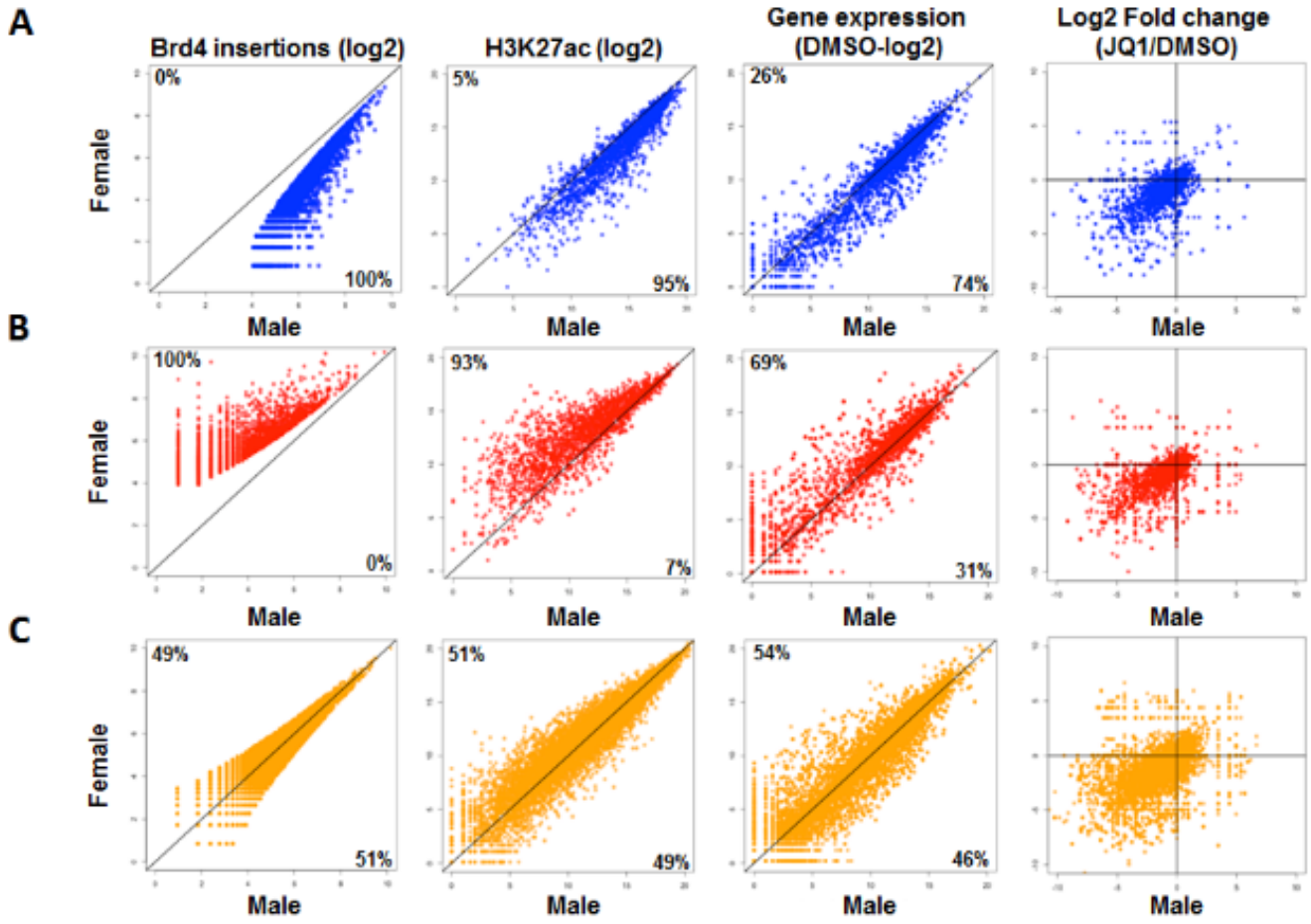

Figure 4. Male and female GBM cells have sexually dimorphic Brd4-bound enhancers and concordant gene expression. Brd4 insertions, H3K27ac signal, and gene expression values (normalized Reads Per Kilobase Million (RPKM)) of the nearest gene(s) in male (x-axis) and female (y-axis) GBM astrocytes for male-specific **(A)**, female-specific **(B)**, and shared **(C)** genes are plotted. The percentage of genes enriched in each sex is indicated at the top left (female) and bottom right (male) of each graph. **(Far right column)** Log2 fold changes (Log2FC) of the gene expression value following JQ1 treatment are plotted as above. Most genes are located in the bottom, left quadrant, indicating down regulation of the gene in both sexes following JQ1.

A

Stem cell pathways regulated by sex-specific Brd4-bound enhancers in male and female GBM cells

Pathway description	Adjusted *p*-value	# of Genes
Male GBM Cells:		
Stem cells	0.00E+00	162
Embryonic stem cells	0.00E+00	152
Mesenchymal stem cells	0.00E+00	140
Neural stem cells	2.00E-03	96
Cancer stem cells	0.00E+00	67
Pluripotent stem cells	8.00E-03	48
Stem cell proliferation	1.00E-03	36
Neoplastic stem cells	6.00E-03	35
Stem cell division	5.00E-03	13
Female GBM Cells:		
Mesenchymal stem cells	0.00E+00	128
Neural stem cells	1.00E-03	92
Stem cell proliferation	2.00E-03	27

B

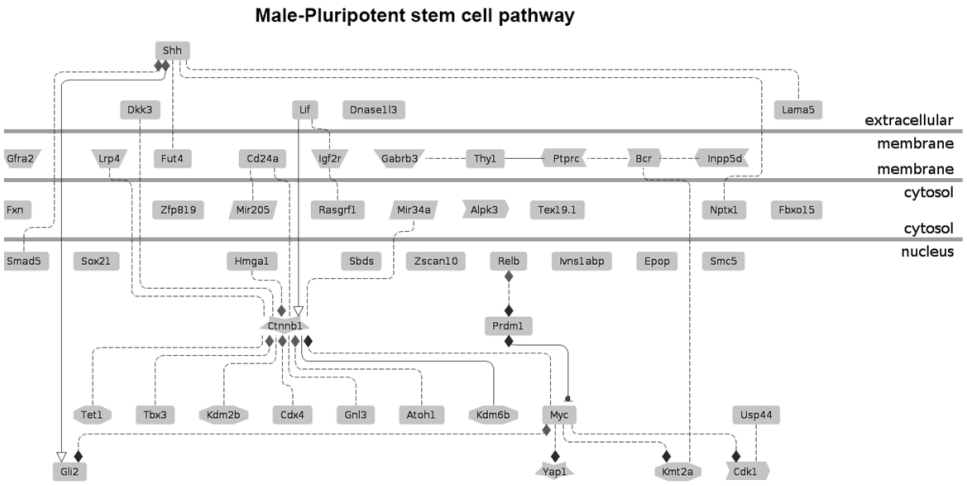

C

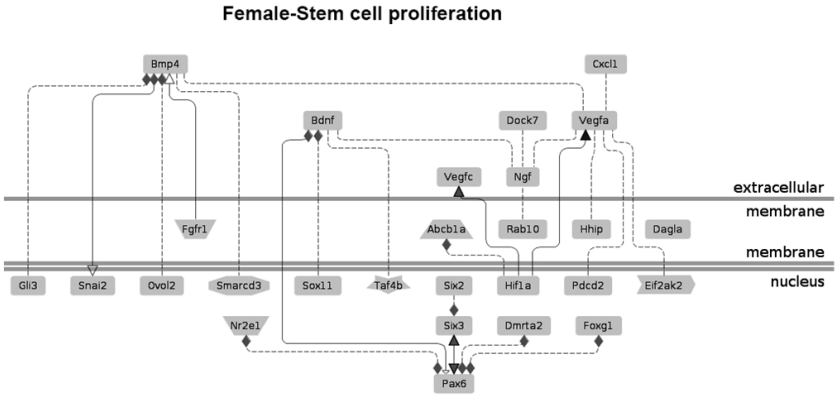

D

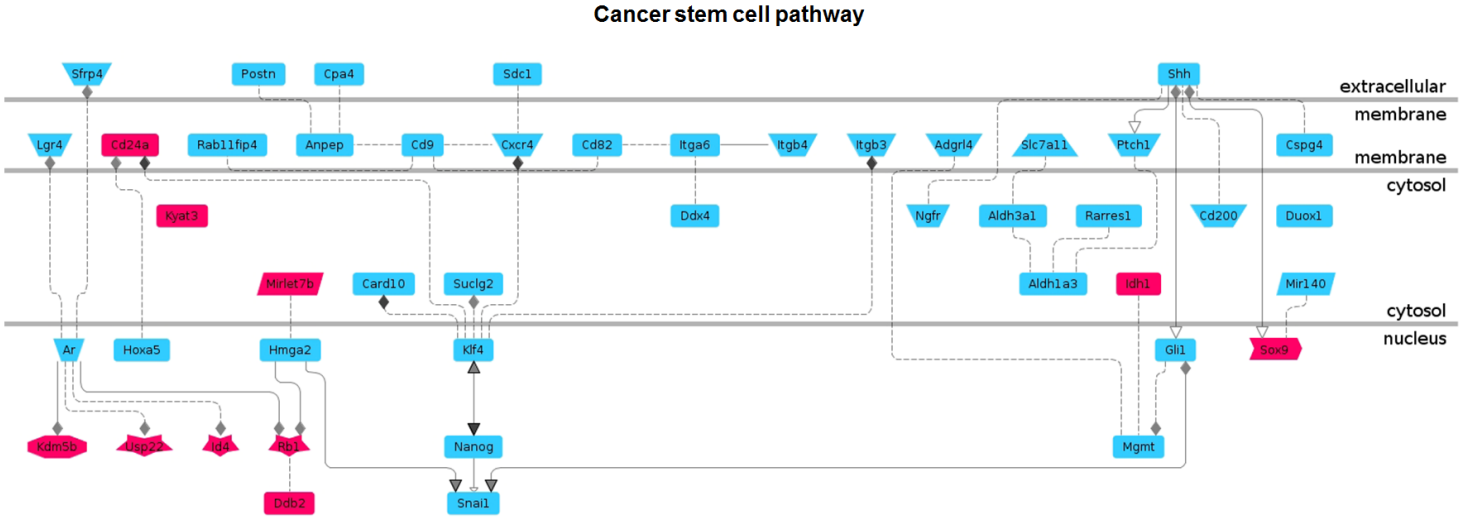

Figure 5. Stem cell pathways regulated by sex-specific Brd4-bound enhancers. (A) Pathway analysis of sex-specific Brd4-bound enhancers in male and female GBM astrocytes revealed an enrichment of stem cell pathways. Male GBM cells were highly enriched for cancer, neoplastic and pluripotent stem cell pathways while female GBM cells were mainly enriched for neural stem cell pathways. Representative examples of these enriched pathways in male **(B)** and female **(C)** GBM astrocytes. Male-specific genes in stem cell pathways included oncogenes such as Myc, Tet1 and Lif while female-specific genes included tumor suppressors such as Six 2 and Six 3. **(D)** Pathway analysis on sex-specific Brd4 regulated genes revealed that the cancer stem cell pathway was significantly affected by JQ1 treatment. Male genes (blue) were downregulated by JQ1 while female genes (red) were upregulated by JQ1.

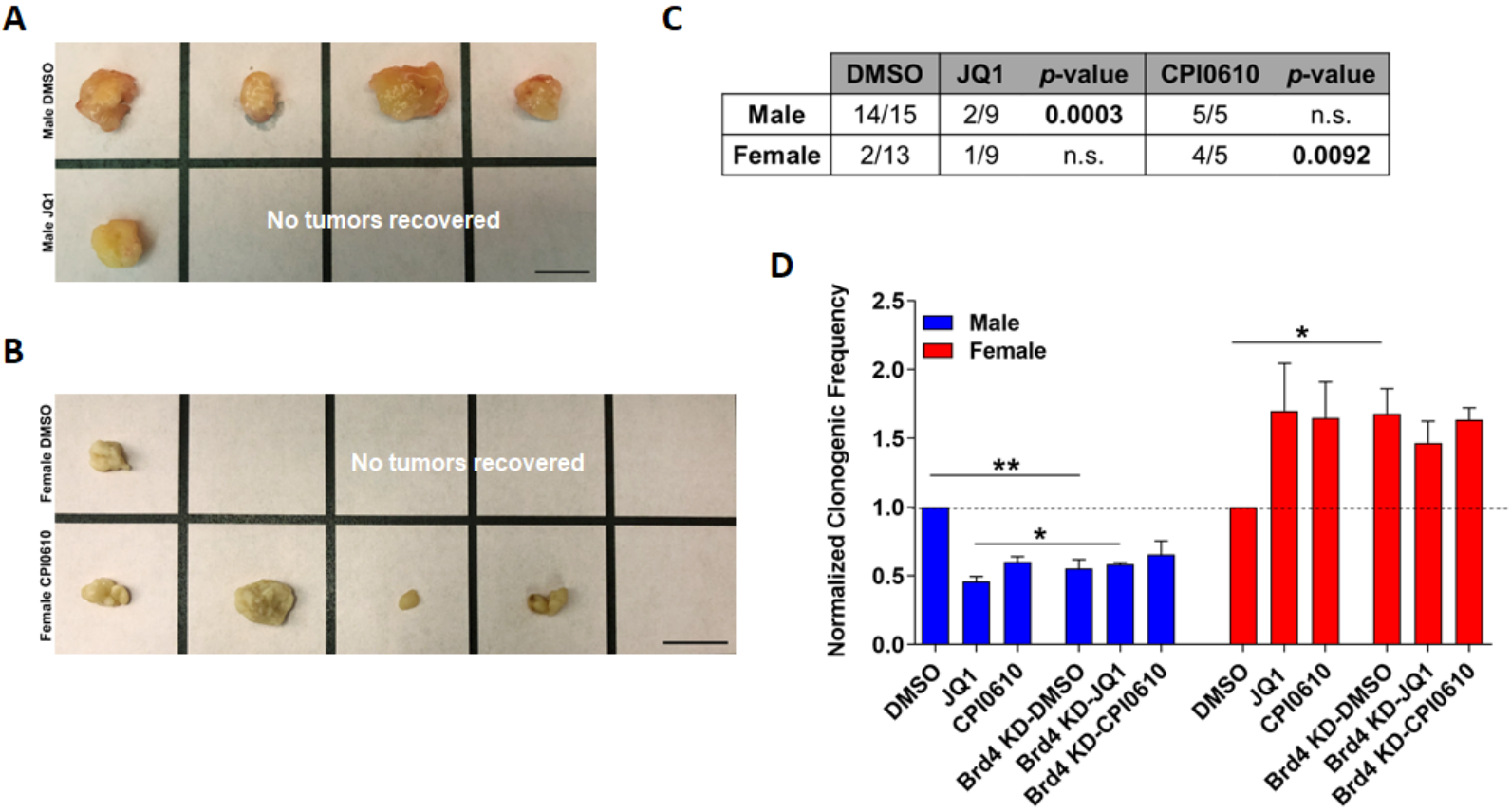

	DMSO	JQ1	*p*-value	CPI0610	*p*-value
Male	14/15	2/9	**0.0003**	5/5	n.s.
Female	2/13	1/9	n.s.	4/5	**0.0092**

Figure 6. BET inhibitors have opposing effects on *in vivo* tumorigenicity in male and female GBM astrocytes. (A) Representative flank tumors from DMSO or JQ1 treated male GBM astrocyte-initiated tumors. **(B)** Representative flank tumors from DMSO or CPI0610 treated female GBM astrocyte-initiated tumors. **(C)** Fraction of male and female GBM cell implants that formed tumors following treatment with DMSO, JQ1 (500 nM), or CPI0610 (1 μM). JQ1-treated male GBM cells were significantly less likely to form tumors than DMSO-treated male GBM cells (Fisher's exact test $p < 0.0003$), while CPI0610-treated female GBM cells were significantly more likely to form tumors than DMSO-treated female GBM cells (Fisher's exact test $p < 0.0092$). **(D)** Normalized clonogenic cell frequency as determined by ELDA assay in male and female GBM cells treated with DMSO or BET inhibitors with or without Brd4 knockdown. No significant change in the effect on clonogenic cell frequency is observed between control and Brd4 knockdown cells treated with BET inhibitors, indicating that Brd4 is the main Brd family member responsible for this sexually dimorphic response to BETi treatment in male and female cells. (*=$p < 0.05$, **=$p < 0.01$ as determined by unpaired two-tailed t-test).

Table 1. Pathway analysis for enriched motifs in male and female GBM cells*

Pathway description	Genes	Adjusted *p*-value	# of Genes
Male GBM Cells: 20 genes/motifs			
Transcription factor activity, sequence-specific DNA binding	Myc, Hoxb4, Max, Pou5f1, Fli1, Klf1, Bach1, Fosl2, Bach2, Nfe2l2, Mafk, Isl1, Nfe2, Jun, Klf5, Fosl1, Batf, Lhx3, Atf3	0.00E+00	19
Neoplastic cell transformation	Myc, Hoxb4, Max, Pou5f1, Fli1, Klf1, Bach1, Fosl2, Bach2, Nfe2l2, Mafk, Nfe2, Jun, Klf5, Klf14, Fosl1, Batf, Lhx3, Atf3	0.00E+00	19
Cell proliferation	Myc, Hoxb4, Fosl2, Isl1, Nfe2, Jun, Fosl1, Atf3	0.00E+00	8
Pluripotent stem cells	Myc, Hoxb4, Max, Pou5f1, Klf1, Mafk, Isl1, Klf5 Egr1, Max, Fosl2, Jun,	0.00E+00	8
Angiogenesis	Nfe2l2, Isl1, Jun, Klf5	0.00E+00	4
Mitogen activated protein kinase signaling	Max, Fosl2, Jun, Fosl1, Atf3	1.10E-02	5
Stem cell differentiation	Pou5f1, Nfe2l2, Isl1, Batf, Hoxb4	0.00E+00	5
Female GBM Cells: 26 genes/motifs			
Transcription factor activity, sequence-specific DNA binding	Mybl1, Rela, Gata4, Ets1, Atf4, Arnt, Maff, Irf1, Smad2, Irf2, Prdm1, Irf3, Ddit3, Ebf1, Smad4, Myod1, Ep300, Irf4, Cebpa, Pgr, Ctcf, Trp53	0.00E+00	22
Growth arrest	Mybl1, Hoxb13, Atf4, Irf1, Smad2, Ddit3, Ebf1, Myod1, Cebpa, Trp53	0.00E+00	10
Negative regulation of cell cycle	Mybl1, Ets1, Irf1, Ddit3, Ep300, Cebpa, Trp53	1.00E-03	7
Histone modification & chromosome organization	Mybl1, Hoxb13, Atf4, Irf1, Smad2, Ddit3, Ebf1, Myod1, Cebpa, Trp53	1.00E-03	6
Cyclin dependent kinase inhibitor 1 signaling	Hoxb13, Irf1, Myod1, Trp53	1.00E-03	4
Estrogen receptor signaling	Hoxb13, Arnt, Irf4, Pgr	3.00E-03	4

* Subset of enriched pathways for enriched motifs in male and female GBM cells

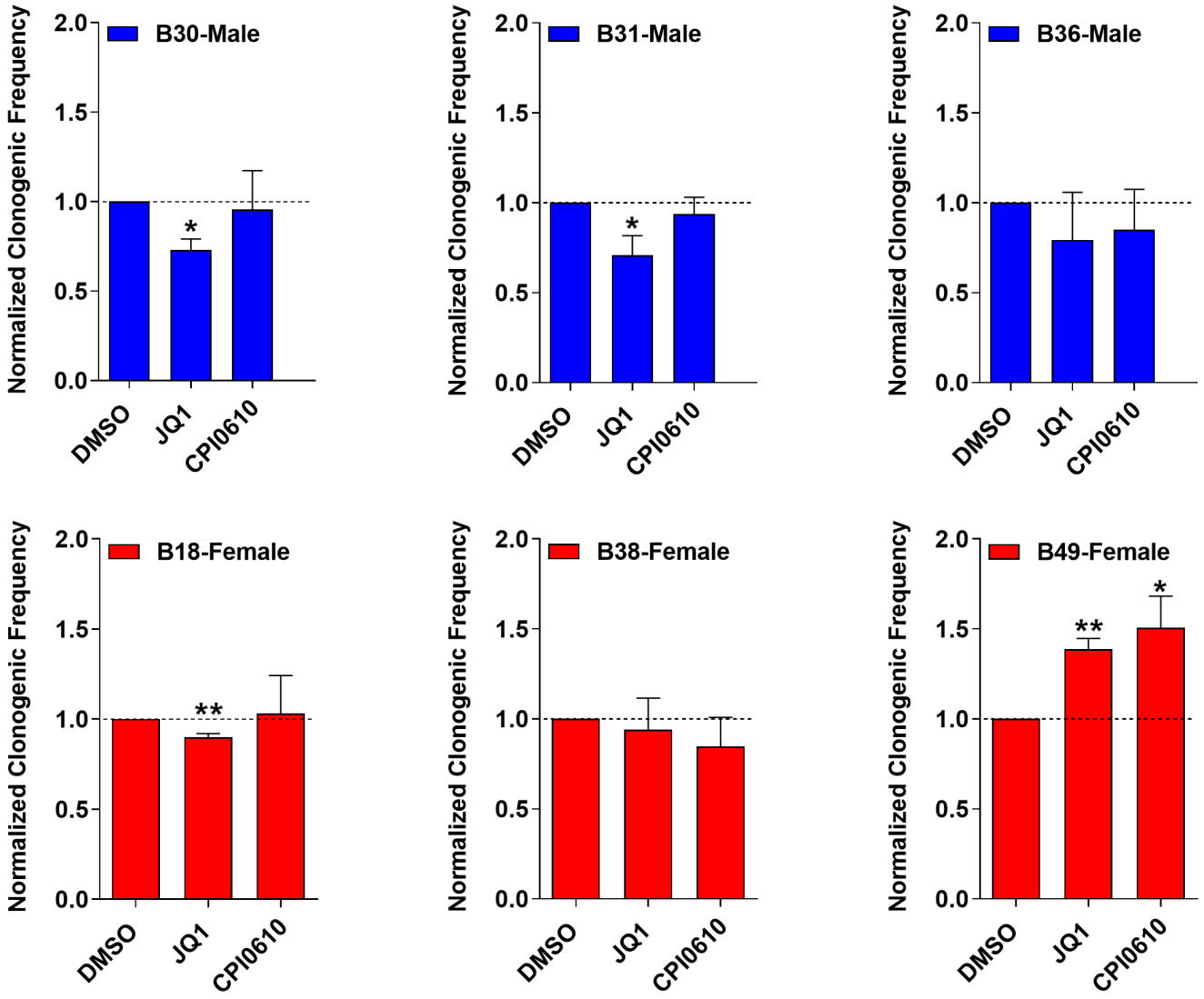

Figure 7. Sex-specific response to BET inhibition treatment and sex-specific Brd4-regulated genes are evident in human primary GBM cells and GBM patients. Normalized clonogenic cell frequency as determined by ELDA assay in male (top panel) and female (bottom panel) human primary GBM cells treated with DMSO (control) JQ1 or CPI0610. JQ1 treatment significantly reduced clonogenic cell frequency in male cells, and significantly increased clonogenic cell frequency in 1 out of 3 female cells. CPI0610 treatment had a similar response pattern as JQ1 in male and female human GBM primary cells. (*=p <0.05, **=p <0.01 as determined by unpaired two-tailed t-test).

Supplementary Materials

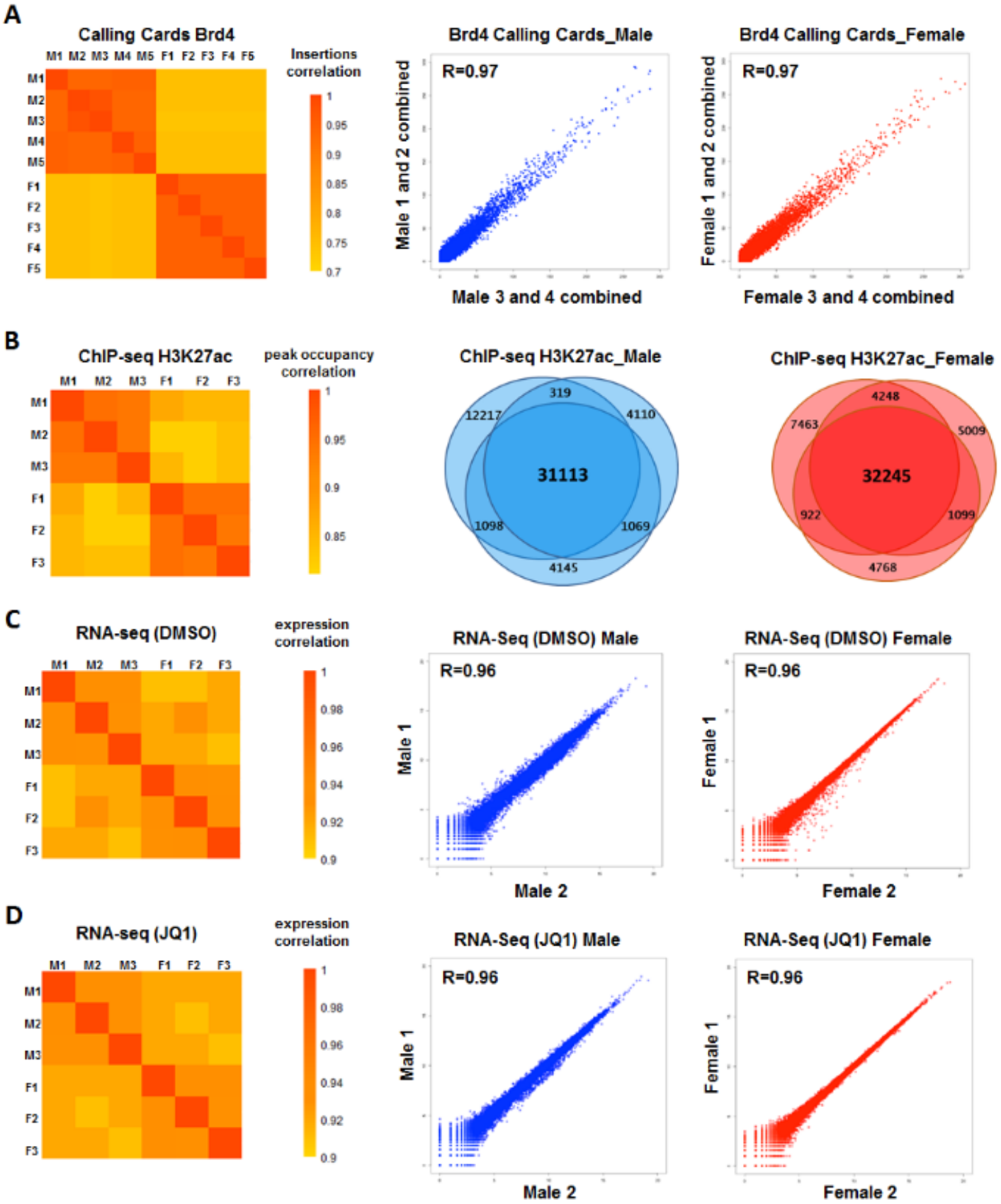

Supplemental Figure 1. Quality assessment of transposon Calling Card, H3K27ac ChIP-seq and RNA-seq experiments. Correlation heatmaps for transposon Calling Card **(A)**, H3K27ac ChIP-seq **(B)** and RNA-seq **(C, D)** were prepared using replicates of male and female GBM samples. Venn diagrams in **(B)** depict the shared H3K27ac-enriched peaks among replicates in male and female GBM cells.

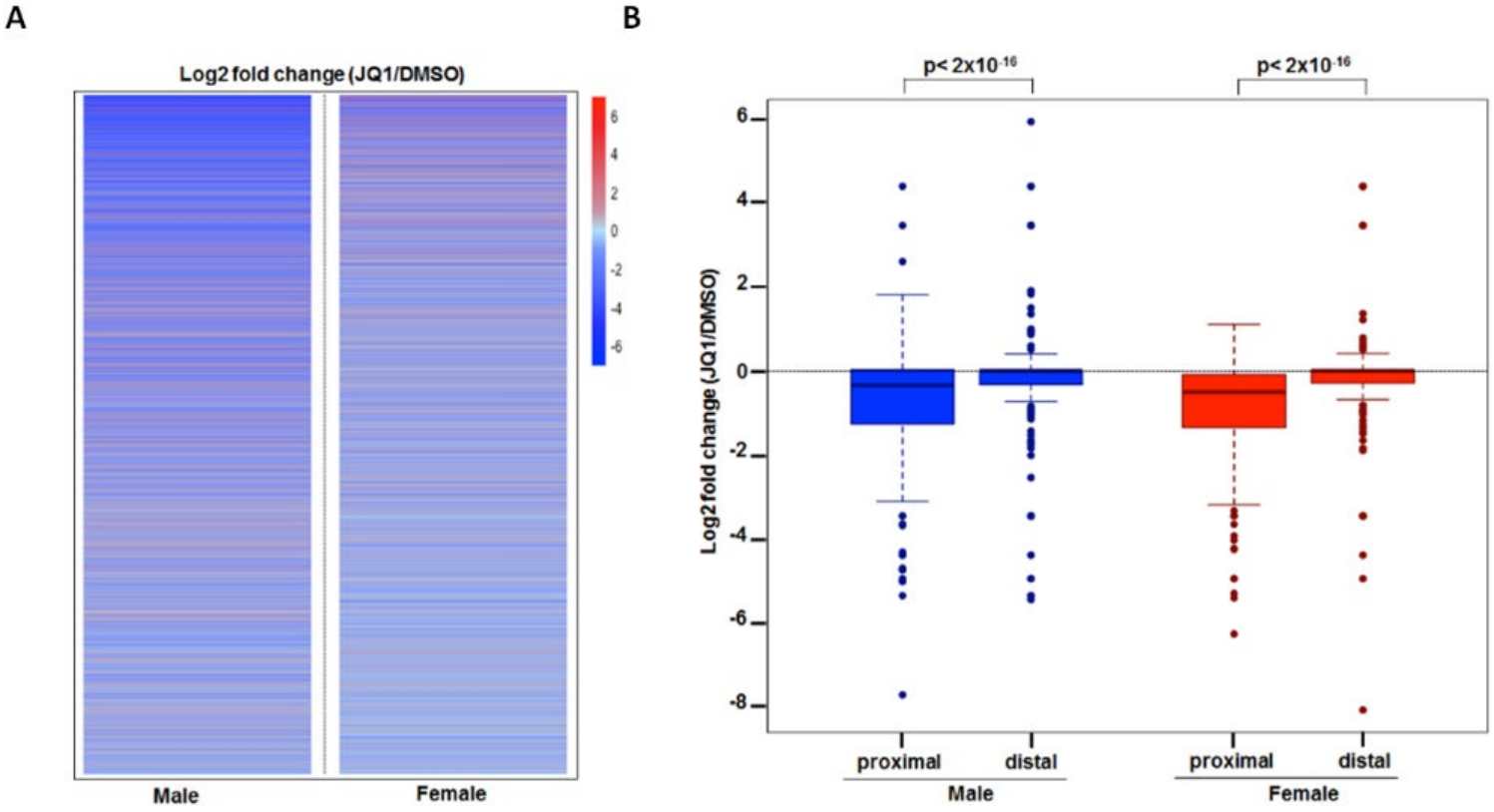

Supplemental Figure 2. **JQ1 effect on gene expression in male and female GBM cells**. **(A)** Heat map of gene expression changes (log2; upregulated in red and downregulated in blue) upon JQ1 treatment in male and female GBM cells **(B)** Boxplot of gene expression changes (log2) of Brd4 proximal and distal genes following JQ1 treatment of male (blue) and female (red) GBM cells. The gene expression profile of genes in close proximity toBrd4 binding sites is compared to distal genes by a Mann-Whitney-Wilcoxon test. Brd4 proximal genes are significantly downregulated compared to Brd4 distal genes in both male and female GBM cells following JQ1 treatment ($p < 2x10^{-16}$).

Supplementary Table 1. Pathway enrichment analysis for sex-specific Brd4-regulated genes in male and female GBM cells as identified by Brd4 calling cards and H3K27ac ChIP_seq*

Pathway description	Adjusted *p*-value	# of Genes
Male GBM Cells: 1740 genes		
Glioblastoma	0.00E+00	349
Cell proliferation	0.00E+00	224
Cell cycle	0.00E+00	152
Regulation of transcription	0.00E+00	113
Tumor angiogenesis	5.00E-03	70
Cancer stem cells	0.00E+00	41
Epidermal growth factor receptor signaling	2.00E-03	15
Female GBM Cells: 1604 genes		
Cell differentiation	0.00E+00	386
Glioblastoma	0.00E+00	320
Regulation of transcription	0.00E+00	181
Cell migration	0.00E+00	161
Neural stem cells	0.00E+00	72
Negative regulation of angiogenesis	1.00E-03	13
Kinase suppressor of Ras	1.00E-03	8

*Subset of pathway enrichment analysis

Supplementary Table 2. Pathway analysis for sex-specific Brd4-bound enhancer genes downregulated following JQ1 treatment in male and female GBM cells*

Pathway description	Subset of Genes	Adjusted *p*-value	# of Genes
Male GBM Cells: 330 genes			
Metabolic Diseases	Nupr1, Nrxn1, Tgfbi, Lgals2, Igfbp3, Mical1, Il33, Prcp, Ly6c1, Bdh2, Crhr1, Slc5a7, Aipl1, Kcnab1, Itgb2, Scd1, Sirt5, Kcnk10, Pax9, Nfatc2, Pcolce2, Pld2, Foxo6, Adh7, Slc16a7, Trhr, Btbd3, Ptx3, Matn2, Shh, Slit3, Fundc1, Foxl1, Ank2, Sspn, Traf1, Cngb1, Apln, C1qtnf1, Decr1, Fbxo7, Fbn2, Chst1, Aqp5, Ptgfr, Ets2, Edil3, Akap6, Nrn1, Lgals3, Mark1, Adam22, Fars2, Ano1, Neu2, Faim2, Fbln1, Kcna4, Rasgrf1, Col25a1, Map2k6, Ar, Arntl, Alk, Car2, Pde1b, Mapk10, Cd38, Aldh3a1, Slc7a7, Aldh1a3, Camk1d, Cdkn2b,Nf1, Cdk6, Cxcl14, Rad51d, Stat6, Pde8a	0.00E+00	200
Chromosome aberrations	Nrxn1, Nalcn, Adssl1, Nup210, Klf12, Crhr1, Itgb2, Scd1, Pax9, Nfatc2, Plscr2, Ctnnd2, Cntnap4, Ptx3, Cradd, Shh, Slit3, Foxl1, Ank2, Traf1, Nhs, Crabp1, Fbn2, Ptgfr, Ets2, Pcyt1b, Akap6, Nrn1, Lgals3, Fars2, Ano1, Neu2, Fbln1, Bcl3, Gria1, Lsp1, Sfrp2, Kcnn3, Chst3, Dap, Dock8, Nov, Fgfbp1, Irak4, Tcn2, Spp1, Alk, Car2, Syn3, Sgca, Mapk10, Tenm4, Cdh23, Nrp2, Nanog, Grpr, Lef1, Zhx2, Flii, Cbr2, Mecom, Nox4, Sema5a, Cyb5a, Fgd2, Socs1, Nf1, Trib2, Cdk6, Rad51d, Stat6, Steap3, Ndp, Eps8, Sh2d4a, Gipc2, Epha3, Ndst3, Nptx1, Ank	2.00E-03	132
Glioma/Glioblastoma	Tgfbi, Nupr1, Igfbp3, Ly6c1, Slc5a7, Eef2k, Itgb2, Nfatc2, Pld2, Adh7, Ctnnd2, Il13ra1, Ptx3, Shh, Apln, Chst1, Ets2, Cd109, Lgals3, Adam22, Ano1, Gria1, Adgrb1, Sall2, Nid1, Sfrp2, Aqp4, Dap, Map2k6, Tcn2, Spp1, Nav3, Ahr, Ar, Il34, Alk, Plxdc1, Nrp2, Nanog, Grpr, Lef1, Xrcc5, Mlkl, Rapgef4, Aldh3a1, Slc7a7, Aldh1a3, Cdkn2b, Nox4, Socs1, Nf1, Lpar1, Cdk6, Thsd4	0.00E+00	130/76
Regulation of transcription	Klf12, Pax9, Nfatc2, Shh, Nrde2, Ets2, Bcl3, Sall2, Sfrp2, Crym, Ahr, Ar, Msx3, Arntl, Mapk10, Nanog, Lef1, Mlip, Zhx2, Xrcc5, Sbno2, Wwp2, Tsc22d3, Bhlhe22, Mecom, Nfatc4, Stat6, Sorbs3	0.00E+00	31
Integrin signaling	Ly6c1, Itgb2, Slit3, Sele, Fbxo7, Edil3, Lgals3, Spp1, Vcam1, Slc7a11, Pde8a, Cd9, Cspg4	7.00E-03	13
Stem cell proliferation	Shh, Fbln1, Sfrp2, Nupr1, Lef1, Mecom, Nf1	4.00E-03	6
Female GBM Cells: 271 genes			
Glioma/Glioblastoma	Rgs4, Sema3e, Mme, Thbs1, Pcdh18, Tnfaip3, Hmmr, Pappa, Vsig2, Ada, Syt1, Acss1, Phex, Galc, Rsad2, Pdgfd, Ngf, Trmt61a, Plcb4, Cdc25a, Ltbp1, Cxcl1, Epha1, Adam12, Wnt5a, Igf1, Grb10, Cxcl12, Lpar4, Trpm3, Angpt2, Ect2, Kif18a, Has2, Adm, Ifih1, F2rl1, Hhip, Ccna1, Nek2, Isg15, S1pr1, Prkaa2, Grin2b, Kif11, Dkk2, Tmem163, Wnt2, Tacr1, Bmpr1b, Usp1, Sulf1, Col3a1, Prps1, Sema3a, Cthrc1, Melk, Hgf, Stc2, Mmp16, Ptprb, Aldh1a1, Usp46, Ptprm, Xbp1, Ptprd, Il7, Pde4b, Ptprz1	0.00E+00	116/75
Chromosome deletion	Mme, Thbs1, Setbp1, Negr1, Pcdh18, Tnfaip3, Pappa, Rhoj, Sox3, Gypc, Ada, Phex, Inhba, Cdh11, Mob3b, Ngf, Pde1a, Plcb4, Epha1, Prepl, Wnt5a, Igf1, Grb10, Gcnt2, Pax2, Alx4, Angpt2, Itga4, En1, Pkp2, Bdh1, Itgb6, Runx1t1, Grin2b, Kif11, Npr3, Wnt2, Boc, Otx2, Bmpr1b, Gja5, Col3a1, Prps1, Sema3a, Magi2, Ripk2, Tg, Tll1, Mmp16, Cftr, Ptprb, Arap2, Aldh1a1, Ptprm, Casp14, Dcn, Ptprd, Cacna1c, Acp6, Etv4, Pde4b, Ptprz1	0.00E+00	71
Immune system process	Raet1e, Thbs1, Sla, Tnfaip3, H60b, Ada, Inhba, Rsad2, Pdgfd, Ifitm3, Oasl2, Il31ra, Cxcl1, Wnt5a, Igf1, Cxcl12, Frk, Angpt2, Ptgs2os, Itga4, Arhgef5, Ifih1, F2rl1, Oasl1, Cysltr1, Masp1, Tacr1, Rrs1, Cftr, Usp46, Ptprd,Acp6, Il7, Pde4b, Ptprz1	0.00E+00	44
Cell cycle	Thbs1, Tnfaip3, Rprd1b, Anapc1, Inhba, Tpx2, Cdc25a, Haus7, Wnt5a, Igf1, Kcnh5, Map9, Kmt5a, Ect2, Kif18a, Cenpw, Map4k3, Cyp26b1, Ckap5, Stk39, Ccna1, Nek2, Kdm8, Smarcd3, Kif11, E2f8, Rrs1, Magi2, Melk, Anapc15	3.00E-03	30
TGF beta signaling	Thbs1, Sema6d, Lox, Inhba, Ltbp1, Adam19, Adam12, Grem2, Gcnt2, Pax2, Cenpw, Has2, Pkp2, Itgb6, Sgcd, Runx1t1, Chrdl1, Bmpr1b, Col3a1, Cthrc1, Melk	3.00E-03	23
Transcription corepressor activity	Sox3, Tbx18, Kmt5a, Runx1t1, E2f8, Jazf1, Lmcd1	1.10E-02	7

* Subset of enriched pathways for sex-specific genes in male and female GBM cells

Supplementary Table 3. Real-time quantitative PCR primers and lentivirus shRNA target sequences

Target	Forward qPCR primer	Reverse qPCR primer	Mouse shRNA target sequence
Mouse Brd2	TGCTGCAAAACGTGACTC	GTAAAGCTGGTACAGAAGCC	CAGCCCAAGAAATCTAAGAAA
Mouse Brd3	GAAAAAGGCTCCCACCAAG	GCTAAGTTGTCGCTTTTCATC	CCTCTCCCTTAGTAACTTGAA
Mouse Brd4	GGAACTTCCTCCCAAAAAGAC	TGCCGCTTCTCCTCATAAG	GCCATCTACACTACGAGAGTT